beneficial effect was explained by the efficient removal of small molecules such as ammonia and glutamine (Gln), which contribute to brain edema along with MMS.[59, 60] Brain edema is a lethal complication of FHF and HDF using high volume of buffers is an essential tool to manage brain edema effectively. We also measured the level of Gln in the discarded buffer and also estimated the distribution volume of Gln. In a patient with an ahepatic state who underwent ALS using over 300 L of buffer, the total amount of removed Gln ranged from 188 947 μmol to 41 165 μmol. The estimated distribution volume of Gln ranged from 30 L to 60 L. There is a significant relationship between total buffer volume and estimated distribution of Gln. Huge amount of buffer can remove huge amount of Gln.[61] These results indicate that HDF using high-volume buffer can remove Gln not only from extracellular fluid but from intracellular fluid. Under the HDF using high-volume buffers, monitoring of intracranial pressure and cerebral blood flow becomes unnecessary. It also provides the clinician with enough time to judge whether liver transplantation is indicated and can avoid unnecessary liver transplantation.

Consensus in Japan was reached at the recent symposium of the Japanese Society for Apheresis held in Ohtsu, Shiga on July 28, 2006 that the effectiveness of the ALS system depends on the volume of buffer used, regardless of whether HDF is performed rapidly or continuously. In addition to the successful 114-day sustainment of a patient with subacute FHF non-A~non-B infection, whose liver failure was judged to be as severe as an hepatic state because of the loss of bilirubin conjugation capacity and urea cycle activity, as well as severe liver atrophy (liver weight 210 g at autopsy) (Figure 2),[39] Inoue reported another five patients with hyperacute FHF due to hepatitis B virus infection who were also judged to be ahepatic that were sustained alive for a long term.[62] One patient subsequently received a successful live donor liver transplant.[63] Two similar hyperacute cases have been also reported,[64] suggesting that PE in combination with high-volume HDF can sustain patients with the severest liver failure, comparable to an hepatic state, who otherwise would not survive, until liver transplantation is possible.

These results suggest that PE in combination with high-volume HDF or CHDF is the only reliable ALS system for Japanese clinicians who are routinely attempting to sustain patients with FHF and related severe liver diseases, although the efficacy of the method has not been ascertained by RCT.[55] A small randomized trial comparing low-volume and high-volume buffer for HDF in a safety manner may be helpful to evaluate the effectiveness of the therapy.

Conclusions

PE in combination with high-volume HDF or high-flow CHDF has become a standard ALS system in Japan. It is rare for only one system of ALS to be used throughout one country. The rationale of the system is simple. While PE replenishes depleted plasma components, toxic substances of middle molecular weight are removed more safely and efficiently than other previous methods by HDF or CHDF using high-volume buffers. This treatment system not only sustain the patient in good condition until the liver recovers or an adequate donor is found, but may also make perioperative care simpler.

Riassunto

Sistemi di supporto epatico come trattamento perioperatorio nel trapianto di fegato – prospettiva storica e recenti progressi in Giappone

Una meta-analisi sull'efficacia dei sistemi di supporto epatico artificiale (*artificial liver support*, ALS) nei casi di insufficienza epatica fulminante (*fulminant hepatic failure*, FHF) eseguita dal gruppo Cochrane Hepato-Biliary Group ha dimostrato che tutti i sistemi di ALS precedentemente sviluppati erano inefficaci nei pazienti affetti da FHF. Questo supporta la teoria che l'unico trattamento di elezione per la FHF sia il trapianto di fegato immediato. Lo scambio di plasma, in combinazione con emodialisi ad alto volume o emodialisi ad alto flusso continuo utilizzando membrane a pori larghi, che era stato escluso dalla meta-analisi di Cochrane a causa della mancanza di trial di controllo randomizzati, è invece

diventato un sistema ALS standard in Giappone. Questo sistema risulta sicuro e rimuove in maniera efficiente più sostanze tossiche di medio e basso pesa molecolare degli altri metodi, utilizzando grandi volumi di tamponi (più di 200 litri per sessione), con il risultato di un risveglio dal coma nei pazienti con FHF grave comparabile a uno stato anepatico. Questi sistemi di supporto epatico artificiale rappresentano strumenti efficaci per mantenere i pazienti affetti da FHF in una condizione favorevole finché il fegato non riprende la sua funzione o non diventa disponibile un trapianto di fegato.

Parole chiave: Fegato - Insufficienza epatica - Emodiafiltrazione - Scambio di plasma.

References

1. Kjaergard LL, Liu J, Als-Nielsen B, Gluud C. Artificial and bioartificial support systems for acute and acute-on-chronic liver failure: a systematic review. JAMA 2003;289:217-22.
2. Liu JP, Gluud LL, Als-Nielsen B, Gluud C. Artificial and bioartificial support systems for liver failure. The Cochrane Database of Systematic Reviews 2004:Art. No.:CD003628.
3. Redeker AG, Yamahiro HS. Controlled trial of exchange-transfusion therapy in fulminant hepatitis. Lancet 1973;1:3-6.
4. O'Grady JG, Gimson AE, O'Brien CJ, Pucknell A, Hughes RD, Williams R. Controlled trials of charcoal hemoperfusion and prognostic factors in fulminant hepatic failure. Gastroenterology 1988;94:1186-92.
5. He JQ, Chen CY, Deng JT, Qi HX, Zang ZQ, Chen JQ. Charcoal hemoperfusion in the treatment of fulminant hepatic failure. Chinese Crit Care Med 2000;12:105-8.
6. Hughes RD, Pucknell A, Routley D, Langley PG, Wendon JA, Williams R. Evaluation of the BioLogic-DT sorbent-suspension dialyser in patients with fulminant hepatic failure. Int J Artif Organs 1994;17:657-62.
7. Mazariegos GV, Ash SR, Patzer JF. Preliminary results: randomized clinical trial of the BioLogic-DT in treatment of acute hepatic failure (AHF) with coma. Artif Organs 1997;21:43-50.
8. Kramer L, Gendo A, Madl C, Mullen K, Kaminski-Russ K, Zauner C. A controlled study of the BioLogic-DT system in chronic hepatic encephalophathy. Hepatology 1998;28:401.
9. Wilkinson AH, Ash SR, Nissenson AR. Hemodiabsorption in treatment of hepatic failure. J Transpl Coord 1998;8:43-50.
10. Ellis AJ, Hughes RD, Nicholl D, Langley PG, Wendon JA, O'Grady JG, Williams R. Temporary extracorporeal liver support for severe acute alcoholic hepatitis using the BioLogic-DT. Int J Artif Organs 1999;22:27-34.
11. Mitzner SR, Stange J, Klammt S, Risler T, Erley CM, Bader BD, Berger ED *et al.* Improvement of hepatorenal syndrome with extracorporeal albumin dialysis MARS: results of a prospective, randomized, controlled clinical trial. Liver Transpl 2000;6:277-86.
12. Heemann U, Treichel U, Loock J, Philipp T, Gerken G, Malago M, Klammt S *et al.* Albumin dialysis in cirrhosis with superimposed acute liver injury: a prospective, controlled study. Hepatology 2002;36:949-58.
13. Stevens C, Busuttil R, Han S, Baquerizo A, Fair J, Shrestha R *et al.* An interim analysis of phase II/III prospective randomized multicenter controlled trial of the Hepat Assist Bioartificial Liver Support System for the treatment of fulminant hepatic failure (abstract). Hepatology 2001;34:299A.
14. Ellis AJ, Hughes RD, Wendon JA, Dunne J, Langley PG, Kelly JH *et al.* Pilot-controlled trial of the extracorporeal liver assist device in acute liver failure. Hepatology 1996;24:1446-51.
15. Larsen FS, Hansen BA, Jorgensen LG, Secher NH, Bondesen S, Linkis P *et al.* Cerebral blood flow velocity during high volume plasmapheresis in fulminant hepatic failure. Int J Artif Organs 1994;17:353-61.
16. Yoshiba M, Inoue K, Sekiyama K, Koh I. Favorable effect of new artificial liver support on survival of patients with fulminant hepatic failure. Artif Organs 1996;20:1169-72.
17. Kiley JE, Welch HF, Pender JC, Welch CS. Removal of blood ammonia by hemodialysis. Proc Soc Exp Biol Med 1956;91:489-90.
18. Sherlock S. Hepatic coma. Gastroenterology 1961;41:1-8.
19. Lee C, Tink A. Exchange transfusion in hepatic coma: report of a case. Med J Aust 1958;45:40-2.
20. Lepore MJ, Martel AJ. Plasmapheresis in hepatic coma. Lancet 1967;290:771-2.
21. Buckner CD, Clift RA, Volwiler W, Donohue DM, Burnell JM, Saunders FC *et al.* Plasma exchange in patients with fulminant hepatic failure. Arch Intern Med 1973;132:487-92.
22. Freeman JG, Matthewson K, Record CO. Plasmapheresis in acute liver failure. Int J Artif Organs 1986;9:433-8.
23. Inoue N, Yoshiba M, Yamazaki Z, Sakai T, Sanjo K, Okada K *et al.* Continuous flow membrane plasmapheresis utilizing cellulose acetate hollow fiber in hepatic failure. In: Brunner G, Schmidt F, editors. Artificial liver support. Berlin: Springer-Verlag; 1981. p. 175-80.
24. Yoshiba M, Inoue N, Sanjo T, Yamazaki Z, Okada Y, Oda T. Plasmapheresis in acute liver failure. In: Nose Y, Malchelsky P, Smith J, Krakauer R, editors. Plasmaphersis therapeutic applications and new techniques. New York, NY: Raven Press; 1983. p. 399-406.
25. Clemmesen JO, Kondrup J, Nielsen LB, Larsen FS, Ott P. Effects of high-volume plasmapheresis on ammonia, urea, and amino acids in patients with acute liver failure. Am J Gastroenterol 2001;96:1217-23.
26. Yoshiba M, Yamada H, Yoshikawa Y, Fujiwara K, Toda G, Oka H, Sanjo T *et al.* Hemodiafiltration treatment of deep hepatic coma by protein passing membrane: case report. Artif Organs 1986;10:417-9.
27. Sadahiro T, Hirasawa H, Oda S, Shiga H, Nakanishi K, Kitamura N *et al.* Usefulness of plasma exchange plus continuous hemodiafiltration to reduce adverse effects associated with plasma exchange in patients with acute liver failure. Crit Care Med 2001;29:1386-92.
28. Schechter DC, Nealon TF Jr, Gibbon JH Jr. A simple extracorporeal device for reducing elevated blood ammonia levels: preliminary report. Surgery 1958;44:892-7.
29. Gazzard BG, Weston MJ, Murray-Lyon IM, Flax H, Record CO, Williams R *et al.* Charcoal haemoperfusion in the treatment of fulminant hepatic failure. Lancet 1974;1:1301-7.
30. Yamazaki Z, Fujimori Y, Sanjo K, Kojima Y, Sugiura M, Wada T *et al.* New artificial liver support (Plasma perfusion detoxification) for hepatic coma. Artif Organs 1977;2:273-6.
31. Sakai T, Fujiwara K, Yoshiba M, Torii M, Hayashi S, Takatsuki K *et al.* Treatment of fulminant hepatitis with charcoal plasma perfusion. Saishin Igaku 1979;34:2542-7.

32. Yoshiba M, Sanjo K, Yamazaki Z, Inoue N, Sakai T, Okada Y. Aggravation of coagulation abnormality by charcoal plasma perfusion in dogs with experimental acute liver failure. Acta Hepatol Jpn 1983;24:426-31.
33. Novelli G, Rossi M, Pretagostini R, Poli L, Novelli L, Berloco P *et al.* MARS (Molecular Adsorbent Recirculating System): experience in 34 cases of acute liver failure. Liver 2002;22(Suppl 2):43-7.
34. Tan HK. Molecular adsorbent recirculating system (MARS). Ann Acad Med Singapore 2004;33:329-35.
35. Opolon P. Significance of middle molecules in the pathogenesis of hepatic encephalopathy. In: Kleinberger G, editor. Advances in hepatic encephalopathy and urea cycle diseases. Basel: Karger; 1984. p. 310-3.
36. Denis J, Opolon P, Nusinovici V, Granger A, Darnis F. Treatment of encephalopathy during fulminant hepatic failure by haemodialysis with high permeability membrane. Gut 1978;19:787-93.
37. Silk DB, Trewby PN, Chase RA, Mellon PJ, Hanid MA, Davies M *et al.* Treatment of fulminant hepatic failure by polyacrylonitrile-membrane haemodialysis. Lancet 1977;2:1-3.
38. Kunitomo T. Development of new artificial kidney systems (Carl W. Walter). Am J Surg 1984;148:594-8.
39. Yoshiba M, Sekiyama K, Iwamura Y, Sugata F. Development of reliable artificial liver support (ALS) — plasma exchange in combination with hemodiafiltration using high-performance membranes. Dig Dis Sci 1993;38:469-76.
40. Inaba S, Kishikawa T, Zaitsu A, Ishibashi H, Kudo J, Ogawa R, Yoshiba M. Continuous haemoperfusion for fulminant hepatic failure. Lancet 1991;338:1342-3.
41. Iizuka K, Kanesaka S, Akizawa T, Niikura K, Kadokawa M, Takahashi Y *et al.* Artificial liver support for the treatment of fulminant viral hepatic failure. Jpn J Apheresis 1995;14:43-5.
42. Sekido H, Matsuo K, Takeda K, Ueda M, Morioka D, Kubota T, Tanaka K *et al.* Usefulness of artificial liver support for pretransplant patients with fulminant hepatic failure. Transplant Proc 2004;36:2555-6.
43. Matsubara S, Okabe K, Ouchi K, Miyazaki Y, Yajima Y, Suzuki H *et al.* Continuous removal of middle molecules by hemofiltration in patients with acute liver failure. Crit Care Med 1990;18:1331-8.
44. Yonekawa C, Nakae H, Tajimi K, Asanuma Y. Effectiveness of combining plasma exchange and continuous hemodiafiltration in patients with postoperative liver failure. Artif Organs 2005;29:324-8.
45. Nakae H, Yonekawa C, Wada H, Asanuma Y, Sato T, Tanaka H. Effectiveness of combining plasma exchange and continuous hemodiafiltration (combined modality therapy in a parallel circuit) in the treatment of patients with acute hepatic failure. Ther Apher 2001;5:471-5.
46. Nakae H, Asanuma Y, Tajimi K. Cytokine removal by plasma exchange with continuous hemodiafiltration in critically ill patients. Ther Apher 2002;6:419-24.
47. Eiseman B, Liem DS, Raffucci F. Heterologous liver perfusion in treatment of hepatic failure. Ann Surg 1965;162:329-45.
48. Demetriou AA, Brown RS Jr, Busuttil RW, Fair J, McGuire BM, Rosenthal P *et al.* Prospective, randomized, multicenter, controlled trial of a bioartificial liver in treating acute liver failure. Ann Surg 2004;239:660-7; discussion 667-70.
49. Millis JM, Cronin DC, Johnson R, Conjeevaram H, Conlin C, Trevino S *et al.* Initial experience with the modified extracorporeal liver-assist device for patients with fulminant hepatic failure: system modifications and clinical impact. Transplantation 2002;74:1735-46.
50. Rozga J, Podesta L, LePage E, Morsiani E, Moscioni AD, Hoffman A *et al.* A bioartificial liver to treat severe acute liver failure. Ann Surg 1994;219:538-44; discussion 536-44.
51. Kuddus R, Patzer JF 2nd, Lopez R, Mazariegos GV, Meighen B, Kramer DJ *et al.* Clinical and laboratory evaluation of the safety of a bioartificial liver assist device for potential transmission of porcine endogenous retrovirus. Transplantation 2002;73:420-9.
52. Mazzoni A, Pardi C, Bortoli M, Uncini Manganelli C, Vanacore R, Urciuoli P, Biancofiore G *et al.* High-volume plasmaexchange: an effective tool in acute liver failure treatment. Int J Artif Organs 2002;25:814-5.
53. Shin K, Nagai Y, Hirano C, Kataoka N, Ono I, Yamamura E *et al.* Survival rate in children with fulminant hepatitis improved by a combination of twice daily plasmapheresis and intensive conservative therapy. J Pediatr Gastroenterol Nutr 1989;9:163-6.
54. Biancofiore G, Bindi LM, Urbani L, Catalano G, Mazzoni A, Scatena F *et al.* Combined twice-daily plasma exchange and continuous veno-venous hemodiafiltration for bridging severe acute liver failure. Transplant Proc 2003;35:3011-4.
55. Chapman RW, Forman D, Peto R, Smallwood R. Liver transplantation for acute hepatic failure? Lancet 1990;335:32-5.
56. Peters RL. Viral hepatitis: a pathologic spectrum. Am J Med Sci 1975;270:17-31.
57. Fujiwara K. The annual report of fulminant hepatitis and late onset hepatic failure 1998-2003. The report from the Committee for Intractable Liver Diseases supported by the Ministry of Health and Labor of Japan 2005;93-107.
58. Sadamori H, Yagi T, Inagaki M, Shima Y, Matsuda H, Tanaka N *et al.* High-flow-rate haemodiafiltration as a brain-support therapy proceeding to liver transplantation for hyperacute fulminant hepatic failure. Eur J Gastroenterol Hepatol 2002;14:435-9.
59. Butterworth RF. Brain edema in acute liver failure. Indian J Gastroenterol 2003;22(Suppl 2):S59-61.
60. Norenberg MD, Rao KV, Jayakumar AR. Mechanisms of ammonia-induced astrocyte swelling. Metab Brain Dis 2005;20:303-18.
61. Inoue K, Kourin A, Watanabe T, Yamada M, Yasuda H, Yoshiba M. Plasma exchange in combination with online-hemodiafiltration as a promising method for purifying the blood of fulminant hepatitis patients. Hepatol Res [In press]
62. Inoue K, Yoshiba M. Apheresis treatment of hyperacute type of fulminant hepatitis. Japanese Journal of Apheresis 2006;25(Suppl.):72.
63. Inoue K, Yoshiba M. Liver transplantation and apheresis treatment in the treatment of fulminant hepatic failure. Japanese Journal of Apheresis 2006;25(Suppl.):109.
64. Inoue J, Ueno Y, Kanno N, Anzai H, Kondo Y, Moritoki Y *et al.* Living related liver transplantation for acute fulminant hepatitis B: experience from two possible hyper-acute cases. Tohoku J Exp Med 2005;205:197-204.

ELSEVIER

Japanese-Style Intensive Medical Care Improves Prognosis for Acute Liver Failure and the Perioperative Management of Liver Transplantation

K. Inoue, T. Watanabe, N. Maruoka, Y. Kuroki, H. Takahashi, and M. Yoshiba

ABSTRACT

The Japanese style of intensive medical care for acute liver failure has yielded high survival rates. The care system comprises artificial liver support (ALS) together with treatment for the underlying disease. Plasma exchange in combination with high-volume hemodiafiltration using an high performance membrane has become the standard ALS system. It is safe, efficiently removing more low and middle molecular weight toxic substances than other methods because of the large volumes of buffer (more than 200 L per session), resulting in recovery from coma in patients with severe fulminant hepatitis , a status comparable with the ahepatic state. This ALS is therefore an effective tool to sustain patients with fulminant hepatitis in a favorable condition until liver function recovers or liver transplantation becomes available. The accompanying treatment for underlying disease serves to limit the liver destruction that hampers regeneration. The treatment has remarkably improved the prognosis for patients with subacute types of fulminant hepatitis, which generally carry a less favorable prognosis than the acute type. This treatment system thus provides more time for physicians to assess the indications for liver transplantation as well as giving the patient a greater chance of undergoing transplantation.

THE LIVER has a great capacity for regeneration, matched only by bone marrow and skin. Vigorous regenerative activity is illustrated by the fact that the liver almost regains its original size within a month after extensive hepatectomy. Thus, living-donor liver transplantation (LDLT) has been successfully performed as an alternative to cadaveric donor liver transplantation (CDLT). In recent years, adult patients with end-stage liver diseases have received grafts containing approximately two thirds of the whole liver.[1]

Fulminant hepatitis (FH) is characterized by sudden, severe liver dysfunction leading to coagulopathy and hepatic encephalopathy despite no known underlying liver disease. In Western countries the onset of coma within 8 weeks from the first sign of symptoms is a widely accepted diagnostic criterion.[2] Many therapeutic efforts have obtained high survival rates in FH, although orthotopic liver transplantation (OLT) including LDLT is currently the only reliable treatment; it results in 60% to 80% survival rates.[3] However, OLT is expensive, and recipients shoulder the adverse effects of life-long immunosuppression. In cases of LDLT, donors also often experience serious physical and mental stress.[4] Furthermore, the increasing incidence of end-stage liver disease has meant that the number of patients awaiting liver transplantation has far outgrown the number of available grafts. Priority for graft distribution has always been based on urgency. Patients with FH are ranked first; therefore, it is essential to avoid unnecessary liver transplantation.

In Japan, intensive medical care for FH was developed originally to meet specific circumstances. The major principle of this care system is an artificial liver support (ALS) system comprising plasma exchange and hemodiafiltration using huge buffer volume.[5] ALS is effective for safely sustaining patients in good condition; Over 90% of patients treated in this fashion regain consciousness.[6] After establishing the ALS, we also developed a treatment regime for the underlying hepatitis, which is often neglected except for

From the Division of Gastroenterology, Showa University Fujigaoka Hospital, Yokohama, Japan.

Address reprint requests to Kazuaki Inoue, MD, PhD, Showa University Fujigaoka Hospital, 1-30 Fujigaoka, Aoba-ku 227-8501, Yokohama, Japan. E-mail: kazu-inoue@med.showa-u.ac.jp

0041-1345/–see front matter
doi:10.1016/j.transproceed.2010.09.073

Table 1. Survival Rate of Fulminant Hepatitis by Intensive Medical Care

Type \ Cause	HAV, n (%)	HBV (acute), n (%)	HBV (carrier), n (%)	Non-A~Non-G, n (%)	Drug, n (%)	Autoimmune Hepatitis (AIH), n (%)	Total, n (%)
Hyper-acute		0/3 (0)					0/3 (0)
Acute	17/18 (94)	15/18 (83)	0/1 (0)	3/4 (75)	1/1 (100)		36/42 (86)
Subacute	1/1 (100)	3/3 (100)	10/11 (91)	14/22 (64)	2/4 (50)	2/4 (50)	32/45 (71)
Subtotal	18/19 (95)	18/24 (75)	10/12 (83)	17/26 (65)	3/5 (60)	2/4 (50)	68/90 (76)
LOHF			1/1 (100)	5/12 (42)	1/1 (100)	1/2 (50)	8/16 (50)
Severe acute hepatitis	6/6 (100)	10/10 (100)	15/15 (100)	14/16 (86)	4/4 (100)	2/2 (100)	51/53 (96)
Total	26/28 (93)	28/36 (78)	34/64 (53)	36/54 (67)	8/10 (80)	5/8 (63)	137/200 (69)

NOTE: One of 3 hyper-acute type underwent living donor liver transplantation and survived. Four of 13 patients with fulminant hepatitis subacute type who failed to respond intensive medical care underwent living donor liver transplantation and 2 of 4 survived.
HAV, hepatitis A virus; HBV, hepatitis B virus; LOHF, late-onset hepatic failure.

the administration of N-acetylcysteine (NAC) in cases of paracetamol intoxication. When liver destruction is progressive or persistent, the liver never regenerates despite its inherent regenerative capability.[7]

Herein, we have reported excellent outcome of the Japanese intensive medical care system for patients with FH. This study also evaluated physicians' ability to assess indications for OLT in FH to ensure appropriate use of the limited organs available.

PATIENTS AND METHODS

Our study group of 159 patients comprised 90 cases of FH, 16 of late-onset hepatic failure (LOHF), and 53 of severe acute hepatitis (SAH). FH was defined by the development of coagulopathy (equal to or less than 40% of prothrombin time) and hepatic encephalopathy (HE; grade II or greater) within 8 weeks of symptom onset among patients without a known underlying liver disease. Development of HE within 10 days was defined as FH acute type and, after 11 days, as FH subacute type. We also defined a FH hyper-acute type, namely liver failure comparable with an ahepatic state that developed within 5 days of the initial symptom. The ahepatic state was characterized by severe impairment of urea cycle and bilirubin conjugation, requiring a blood urea nitrogen less than 1 mg/dL and direct bilirubin to total bilirubin ratio less than 0.1. LOHF was defined by the development of the same HE and coagulopathy as FH within 8 to 24 weeks of symptom onset. SAH was defined by the same coagulopathy as FH but without or with grade I HE (Table 1). Immediately after the onset of hepatic coma, patients were placed on ALS involving plasma exchange and hemodiafiltration using high-performance membranes and huge volumes of buffer (Fig 1). Treatment for underlying hepatitis consisted of immunosuppressive therapy using a methylprednisolone pulse followed by withdrawal and continuous infusion of cyclosporine (Fig 2). Antiviral treatment comprised interferon beta (IFN-β) and/or Entecavir (ETV). The indication for IFN-β was a patient whose underlying disease entailed persistent viral replication including indeterminate cases when autoimmunity or drugs had been excluded as the etiology. The indication for ETV was a

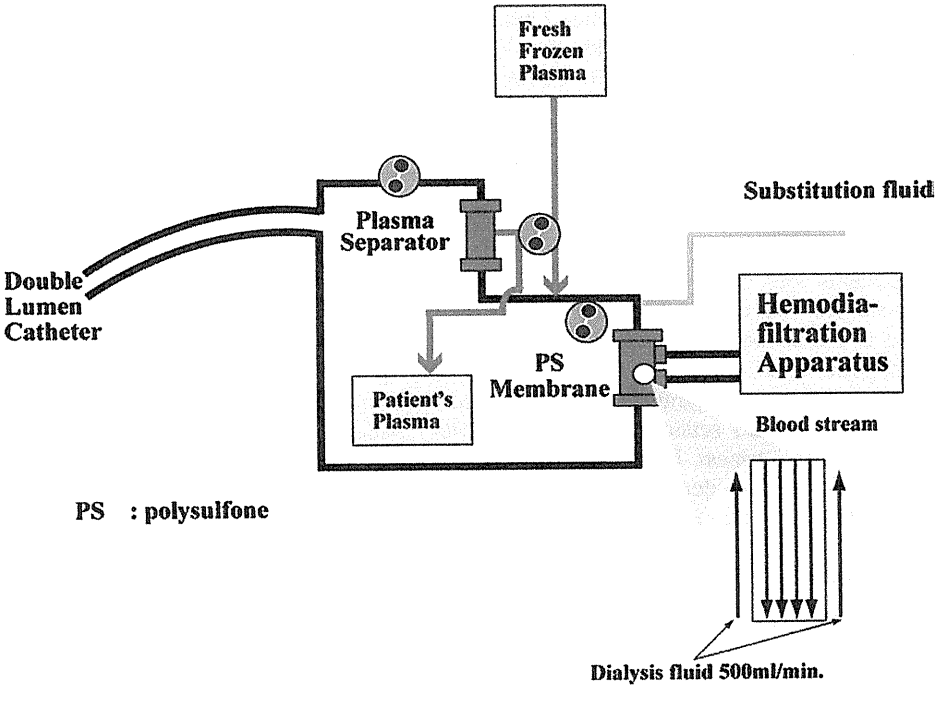

Fig 1. Circuit diagram of plasma exchange in combination with hemodiafiltration using high-performance polysulfone membrane. Substitution fluid comprising ultra-pure water and high-quality concentrate was infused in the predilution mode at 15 to 20 L/h concomitantly with dialysate at a flow rate of 500 mL/min. The substitution fluid was supplied through a hygienic flow path. The hemodiafilter used was Toraysulfone TS-BP1.8L (Toray Medical Co, Tokyo, Japan). The anticoagulant for the artificial liver support was nafamostat mesilate (Futhan; Torii, Tokyo, Japan) at a priming dose of 30 mg and at a continuous dose of 30 mg/h.

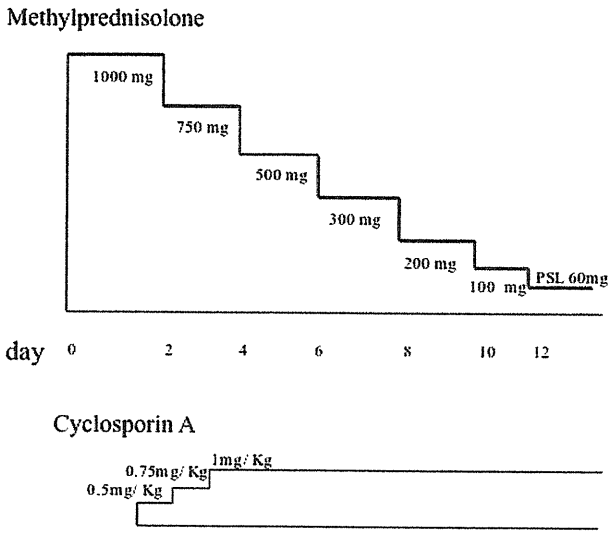

Fig 2. Immunosuppressive protocol comprised a methylprednisolone pulse followed by a slow withdrawal and continuous infusion of cyclosporin A. The target level of cyclosporin A was 250 to 350 ng/mL.

patient whose underlying disease was persistent hepatitis B virus (HBV) replication (Fig 3).

RESULTS

Of the 90 FH cases, 3 were the hyper-acute type; all had acute hepatitis B virus (HBV) infections and had progressed to severe liver failure comparable with an ahepatic state. They were immediately placed on ALS including PE and HDF, which sustained them in a good condition. One of the 3 patients subsequently survived LDLT. Although the ALS system sustained the other 2 patients in favorable condition for more than 2 weeks, they subsequently died because an organ donor could not be found.

Other FH cases included 42 acute-type FH, most of whom had acute infections with hepatitis A virus or HBV; among them, 36/42 (86%) survived ALS. The remaining 45 patients were FH subacute type with 32 (71%) surviving after placement on the ALS system and undergoing treatment for the underlying liver disease. Among the remaining 13 patients four underwent LDLT and 2 were survivors. The survival rate of LOHF patients under the same treatment as FH subacute type was 50% (8/16). Among the 53 SAH patients, 51 survived (96%) with 2 succumbing to a fungal infection or aggravation of malignant lymphoma. After several ALS sessions, 109 of 116 (94%) patients regained consciousness. The 2-week survival rate was 107 of 116 (92%). Brain edema observed in a few cases was reversible by several sessions of ALS in most cases.

DISCUSSION

We attained high survival rates among FH patients using the Japanese style of intensive medical care. Several blood purification methods have been developed in Japan since the late 1970s. The first method of PE was effective to replenish depleted plasma components, especially coagulation factors, but was of limited effectiveness to remove substances displaying a large body pool such as glutamine (Gln), which causes brain edema.[8] For the efficient, safe removal of low and middle molecular substance with large body pools, we developed HDF using large-pore high-performance membranes. More than 90% of unselected patients treated in this way regained full alertness. Brain edema and renal failure are regarded as destined complications of FHF. They are seen in only a few percent of patients and are mostly reversible. Our ALS system uses more than 200 L of buffer per session to cleanse the patient's blood. Removal of Gln clearly depends on the buffer volume per session. Under HDF using high-volume buffers, monitoring of intracranial pressure and cerebral blood flow becomes unnecessary. This strategy also increases the time for clinicians to judge whether liver transplantation is indicated, thus avoiding unnecessary procedures.

We divided cases of FH into transient and persistent types based on the mode of infection. The Transient type is characterized by a rapid eradication of causal viruses like HAV and acute HBV infection. The persistent type is typified by persistent or even chronic replication of causal viruses such as in HBV carriers because of HCV, HDV, and presumably non-A-non-G virus. Interestingly, the majority of patients with acute type of FH according to the Japanese criteria, namely, coma occurring within 10 days of first onset of symptoms, was of the transient type; whereas most subacute-type FH patients were the persistent type.

Hepatitis treatment differs between the transient and persistent type. In FH acute type, effective ALS causes liver destruction to cease spontaneously with eradication of the causal virus resulting in rapid recovery and survival. Among our 42 patients, 36 patients (86%) survived without liver transplantation. Exceptional cases are the hyper-acute type whose liver progresses into an ahepatic state as exemplified by a rapid loss of direct bilirubin and blood urea nitrogen. PE in combination with HDF was an effective tool to sustain patients in a favorable condition allowing physicians time to find a donor organ. In the present study, 1 patient of this type was fortunate enough to receive an LDLT in time. In the persistent type, which corresponds to the FH subacute condition, liver damage must be limited to prevent destruction beyond the limit of regeneration. In our experience between 1986 and 1993, only 38% of patients with

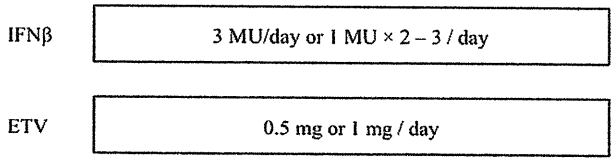

Fig 3. Antiviral treatment comprised interferon β and Entecavir. Interferon β was administered 3 MU daily or 2 or 3 times of 1 MU daily. Entecavir was administered 0.5 mg or 1 mg daily. IFN, interferon; ETV, Entecavir.

the persistent type finally survived despite more than 90% of them regaining full alertness (data not shown). Confronted by this insufficient result, we originally elaborated the treatment to terminate liver destruction of the latter type. Because viral replication is persistent in this type, we have administered IFN universally for cases presumed to be viral hepatitis and a nucleotide/nucleoside analogue for FH because of persistent HBV infection. For the indeterminate cases, we administered IFN on the assumption that it was related to a viral infection of some type. In combination with antivirals, we administer immunosuppressive agents that dampen host cytotoxic immunologic reactions in FH. Figure 2 illustrates the scheme of our immunosuppressive treatment, for which we have already presented some preliminary results.[7] The combination therapy seeks to rapidly reduce transaminase levels. After establishing the treatment for the underlying disease, the survival rate among patients with the persistent type of FH increased to 71% (32/45) in the present study.

In conclusion, The Japanese treatment system remarkably improved the prognosis of acute liver failure. The treatment system sustained patients in good condition until the liver recovered or an adequate donor was found, allowing more appropriate perioperative management and determination of organ allocation.

REFERENCES

1. Liu CL, Fan ST, Lo CM, et al: Right-lobe live donor liver transplantation improves survival of patients with acute liver failure. Br J Surg 89:317, 2002
2. Trey C, Davidson CS: The management of fulminant hepatic failure. Prog Liver Dis 3:282, 1970
3. Sass DA, Shakil AO: Fulminant hepatic failure. Liver Transpl 11:594, 2005
4. Northup PG, Berg CL: Living donor liver transplantation: the historical and cultural basis of policy decisions and ongoing ethical questions. Health Policy 72:175, 2005
5. Inoue K, Kourin A, Watanabe T, et al: Artificial liver support system using large buffer volumes removes significant glutamine and is an ideal bridge to liver transplantation. Transplant Proc 41:259, 2009
6. Yoshiba M, Inoue K, Sekiyama K, et al: Favorable effect of new artificial liver support on survival of patients with fulminant hepatic failure. Artif Organs 20:1169, 1996
7. Yoshiba M: Recent progress in the treatment of fulminant hepatic failure in Japan. J Infect Chemother 4:41, 1998
8. Blei AT: Pathophysiology of brain edema in fulminant hepatic failure, revisited. Metab Brain Dis 16:85, 2001

JOURNAL OF CLINICAL MICROBIOLOGY, Nov. 2010, p. 3843–3851 Vol. 48, No. 11
0095-1137/10/$12.00 doi:10.1128/JCM.00415-10

Detection of Hepatitis B and C Viruses in Almost All Hepatocytes by Modified PCR-Based *In Situ* Hybridization▽

Hideko Nuriya,[1] Kazuaki Inoue,[1,2] Takeshi Tanaka,[3] Yukiko Hayashi,[4] Tsunekazu Hishima,[4] Nobuaki Funata,[4] Kyosuke Kaji,[5] Seishu Hayashi,[3] Shuichi Kaneko,[5] and Michinori Kohara[1]*

Department of Microbiology and Cell Biology, Tokyo Metropolitan Institute of Medical Science, 2-1-6 Kamikitazawa, Setagaya-ku, Tokyo 156-0057, Japan[1]; Division of Gastroenterology, Showa University Fujigaoka Hospital, 1-30 Aoba-ku, Fujigaoka, Yokohama 227-8501, Japan[2]; Liver Unit, Tokyo Metropolitan Komagome Hospital, 3-18-22 Honkomagome, Bunkyo-ku, Tokyo 113-8613, Japan[3]; Department of Pathology, Tokyo Metropolitan Komagome Hospital, 3-18-22 Honkomagome, Bunkyo-ku, Tokyo 113-8613, Japan[4]; and Department of Gastroenterology, Kanazawa University Graduate School of Medical Science, Ishikawa 920-8641, Japan[5]

Received 28 February 2010/Returned for modification 22 April 2010/Accepted 16 August 2010

Although PCR-based *in situ* hybridization (PCR-ISH) can be used to determine the distribution and localization of pathogens in tissues, this approach is hampered by its low specificity. Therefore, we used a highly specific and sensitive PCR-ISH method to reveal the lobular distribution and intracellular localization of hepatitis B virus (HBV) and HCV in chronic liver disease and to clarify the state of persistent HBV and HCV infection in the liver. HBV genomic DNA was detected in almost all hepatocytes, whereas HBV RNA or protein was differentially distributed only in a subset of the HBV DNA-positive region. Further, HCV genomic RNA was detected in almost all hepatocytes and was localized to the cytoplasm. HCV RNA was also detected in the epithelium of the large bile duct but not in endothelial cells, portal tracts, or sinusoidal lymphocytes. In patients with HBV and HCV coinfection, HCV RNA was localized to the noncancerous tissue, whereas HBV DNA was found only in the cancerous tissue. Using this novel PCR-ISH method, we could visualize the staining pattern of HBV and HCV in liver sections, and we obtained results consistent with those of real-time detection (RTD)-PCR analysis. In conclusion, almost all hepatocytes are infected with HBV or HCV in chronic liver disease; this finding implies that the viruses spreads throughout the liver in the chronic stage.

Hepatitis B virus (HBV) and hepatitis C virus (HCV) are the primary causative agents of chronic liver disease (2, 9, 17). HBV infection remains a global health problem; it is estimated that 350 million individuals are persistently infected with the virus and that approximately 15% to 25% of these individuals will die due to the sequelae of the infection (23, 29). Further, more than 170 million people are infected with HCV worldwide (21). HCV has a single-stranded RNA genome (8, 19), does not have canonical oncogenes, and can easily establish chronic infection without integration into the host genome (3, 20), resulting in hepatic steatosis and hepatocellular carcinoma (HCC) (28). The viruses share a similar route of transmission, such as via the transfusion of infected blood or body fluids or use of contaminated needles.

Several studies have shown that 10% to 35% of the individuals infected with HBV also have HCV infection, although the prevalence varies depending on the population studied (4, 32, 34). The relationship between coinfection and acceleration of malignant transformation remains unclear, but HBV and HCV coinfection seems to alter the natural history of both HBV-related and HCV-related liver disease (2, 12). HCV has been shown to inhibit HBV gene expression (7, 15). The high prevalence of occult HBV infection may indicate that HCV also inhibits HBV replication (34). Most epidemiological studies of HBV have been performed by using diagnostic serological assays (16). We recently used a novel, highly sensitive diagnostic PCR method to demonstrate that the HBV genome is detectable in the sera of a substantial proportion of patients with chronic HCV infection who are seronegative for the standard HBV-related markers (1, 34). Further, we reported the levels of HBV DNA and HCV RNA in cancerous and noncancerous liver tissue using real-time detection (RTD)-PCR (34). RTD-PCR is an accurate assay method, but it can determine the levels of genomic DNA and RNA only in homogenized tissue. In this study, we developed a PCR-based *in situ* hybridization (PCR-ISH) method for detecting and visualizing HBV DNA, HBV RNA, and HCV RNA and comparing their protein expression patterns, with the aim to reveal the lobular distribution and intracellular localization of HBV and HCV in chronic liver disease and to clarify the state of persistent HBV and HCV infection in the liver.

MATERIALS AND METHODS

Patients. Twenty-nine patients were admitted to Tokyo Metropolitan Komagome Hospital for the treatment of hepatic tumors. Of these patients, 14 were considered to have chronic HCV infection (persistently positive results for HCV antibody), 8 were diagnosed with chronic hepatitis B (persistently positive results for HBV surface antigen [HBsAg]), and 7 showed negative results for both viral markers but had metastatic liver cancer (6 with colonic cancer and 1 with gastric cancer). We used four samples from seven patients as controls for PCR-ISH and four samples from seven patients as controls for reverse transcriptase PCR (RT-PCR)–ISH (Table 1). Of the 14 patients with chronic hepatitis C, two showed positive results for HBV DNA by RTD-PCR. HBsAg and second-generation HCV antibody were measured by using enzyme-linked immunosor-

* Corresponding author. Mailing address: Department of Microbiology and Cell Biology, The Tokyo Metropolitan Institute of Medical Science, 2-1-6, Kamikitazawa, Setagaya-ku, Tokyo 156-8506, Japan. Phone: 81-3-5316-3232. Fax: 81-3-5316-3137. E-mail: kohara-mc@igakuken.or.jp.

▽ Published ahead of print on 25 August 2010.

TABLE 1. Patient profiles and results of the present study

Patient no.	Age (yr)	Gender[a]	HCV antibody	HBs Ag	Liver histology	RT-PCR–ISH HCV	PCR-ISH HBV	Serum HBV DNA (copies/ml)[b]	Serum HCV RNA		IFN treatment	Note
									Copies/ml	KIU/ml[d]		
1	53	M	−	+	A2F3		+	1.1×10^2			−	
2	42	M	−	+	A2F2		+	4.0×10^5			−	Fig. 2A
3	43	M	−	+	A2F3		+	1.6×10^7			−	
4	53	M	−	+	A2F4		+	6.4×10^3			−	Fig. 1A
5	55	M	−	+	A2F3		+	1.0×10^3			−	Fig. 3A
6	54	M	−	+	A2F4	−	+	NT[c]			−	
7	31	M	−	+	A3F3		+	3.0×10^9			+	
8	61	F	−	+	A3F3		+	NT			−	
9	63	M	+	−	A3F4	+	−		5.6×10^6		−	Fig. 4D
10	56	M	+	−	A2F3	+	−		NT		+	
11	67	F	+	−	A3F4	−	−		NT		−	
12	73	M	+	−	A2F4	+			1.2×10^6		−	Fig. 1B
13	68	F	+	−	A3F4	+			1.1×10^6		−	
14	76	F	+	−	A2F4	+			9.5×10^5		−	Fig. 4A
15	62	M	+	−	A2F3	+			7.2×10^5		−	
16	65	M	+	−	A3F4	+			NT		−	
17	60	F	+	−	A3F4	+				41	−	
18	48	F	+	−	A2F1	+			7.6×10^6	>850	−	Fig. 4C
19	43	M	+	−	A2F3	+				389	−	
20	59	M	+	−	A2F3	+				>850	−	
21	72	F	+	−	A2F4	+	+	3.9×10^1	5.0×10^7			Fig. 5
22	69	M	+	−	A2F3	+	+	5.0×10^1	3.0×10^7			
23	69	M	−	−	Normal	−	−					Gastric cancer
24	58	M	−	−	Normal		−					Colon cancer
25	58	M	−	−	Normal	−						Colon cancer
26	59	F	−	−	Normal	−						Colon cancer
27	65	M	−	−	Normal	−						Colon cancer
28	47	M	−	−	Normal		−					Colon cancer
29	81	F	−	−	Normal		−					Colon cancer

[a] M, male; F, female.
[b] Serum HBV DNA was positive in patients 21 and 22.
[c] NT, not tested.
[d] KIU, kilo international units.

bent assay (ELISA) kits (Abbott Laboratories, Chicago, IL, and International Reagent Corp., Kobe, Japan, respectively). All 29 patients underwent hepatic resection. Histological evaluation of the liver was carried out according to the METAVIR scoring system (3).

Ethical approval. The Institutional Review Board of Tokyo Metropolitan Komagome Hospital approved the study. Written informed consent was obtained from all the subjects.

Sample preparation. The liver tissue samples for HBV DNA detection were fixed in 10% buffered formalin (pH 7.4) for 18 h, embedded in paraffin, cut into 6-μm-thick sections, and mounted on silane-coated glass slides for use with a GeneAmp *in situ* PCR system 1000 unit (Applied Biosystems, Foster City, CA). The slides were washed thrice in xylene for 8 min at each washing, rinsed thrice in 99.5% ethanol and 75% ethanol for 5 min at each rinsing, and rehydrated in distilled water for deparaffinization. For detecting HBV mRNA and HCV RNA, OCT-embedded frozen liver tissue samples were cut into 10-μm-thick sections and mounted on silane-coated glass slides. They were then fixed in 10% buffered formalin (pH 7.4) for 17 to 21 h, rinsed twice in distilled water treated with 0.01% diethylpyrocarbonate (DEPC) for 2 min at each rinse, rinsed in 99.5% ethanol for 1 min, and then air dried and stored at −80°C until use. The tissue sections on the glass slides were digested with proteinase K (1 to 30 μg/ml and 1 to 200 μg/ml for the noncancerous and cancerous regions of the paraffin-embedded sections, respectively; 0.008 to 1.0 μg/ml for the frozen sections) in 50 mM Tris (pH 7.5) at 37°C for 30 min in a humidified chamber. Subsequently, proteinase K was inactivated at 97°C for 10 min, and then the sections were rinsed with distilled water, dehydrated in 99.5% ethanol, and air dried.

Primers and probes for PCR-ISH and RT-PCR–ISH. The primers used to amplify the S and X regions of HBV and the 5′ untranslated region (5′-UTR) of HCV as well as the corresponding probes are listed in Table 2. We created a digoxigenin (DIG)-dUTP tail at the 3′ end of the 5′-DIG probe using a DNA tailing kit (Roche, Basel, Switzerland).

PCR-ISH for detecting HBV DNA. PCR was performed by using one of two sets of antisense and sense primers complementary to the sequences located in the S and X regions of HBV. The PCR mixture contained 10 mM Tris-HCl (pH 8.3), 50 mM KCl, 3.0 mM $MgCl_2$, 0.8 mM each primer, 197 mM deoxynucleoside triphosphates (dNTPs), and 10 U/50 μl *Taq* DNA polymerase (AmpliTaq Gold; Applied Biosystems).

The tissue slides were warmed to 70°C, and 50 μl of the PCR mixture was overlaid onto the proteinase K-treated tissue specimens. An Ampli cover disc with Ampli cover clips (Applied Biosystems) was attached to each specimen. The slides were placed in the GeneAmp *in situ* PCR system 1000 unit at 70°C. PCR was performed at 95°C for 10 min, followed by 35 to 55 cycles at 95°C for 30 s and 60°C for 2 min and a final extension at 72°C for 10 min. Immediately after the PCR, the slides were fixed in 4% paraformaldehyde in phosphate-buffered saline (PBS) for 10 min at 37°C, washed in 2× SSC (1× SSC is 0.15 M NaCl plus 0.015 M sodium citrate) for 2 min, rinsed with distilled water for 2 min, dehydrated in 99.5% ethanol for 1 min, and then air dried. ISH was performed by mixing the DIG-labeled probe (final concentration, 100 ng/ml) with 65 μl of hybridization buffer (50% deionized formamide, 4× SSC, 1× Denhardt's solution [0.2% bovine serum albumin {BSA}, 0.2% polyvinyl pyrrolidone, 0.2% Ficoll 400], 100 μg/ml denatured salmon sperm DNA, 100 μg/ml yeast RNA, and 1 mM EDTA) and then adding the mixture to each section, heating to 97°C for 10 min, and cooling to 37°C in decrements of 1°C/min (27). Hybridization was carried out overnight at 37°C. Stringency washes were conducted with the following: 2× SSC twice for 10 min at 37°C, 0.03× SSC for 10 min at 50°C, 0.1% Triton X-100 in TBS (0.1 M Tris [pH 7.5], 0.1 M NaCl) for 10 min at room temperature, and TBS for 5 min at room temperature. After incubation in blocking reagent (0.1 M Tris

[pH 7.5], 0.1 M NaCl, 10% sheep serum, 3% BSA) at room temperature for 15 min, the slides were covered with 100 μl anti-DIG antibody conjugated with alkaline phosphatase (Roche) and diluted at 1:900 with 1% BSA in TBS at 37°C for 60 min. After this reaction, the slides were washed twice (3 min each) with 0.1% Triton X-100 in TBS, then with TBS alone, and finally with APS (0.1 M Tris [pH 9.0], 0.1 M NaCl, 50 mM $MgCl_2$) at room temperature. The slides were incubated in 100 μl dye solution (338 μg/ml nitroblue tetrazolium chloride [NBT], 175 μg/ml 5-bromo-4-chloro-3-indolyl-phosphate 4-toluidine salt [BCIP], and 450 μM Levamisole [Vector Labs, Burlingame, CA] in APS) at 37°C in the dark. After sufficient color development, they were washed with deionized water for 1 min and then mounted with aqueous mounting medium.

RT-PCR–ISH for detecting HBV RNA. The OCT-embedded frozen sections were placed on glass slides. After proteinase K treatment, the tissue sections were digested with RNase-free DNase I (Roche; diluted to 3 U/μl in 0.1 M sodium acetate and 5 mM $MgSO_4$). The DNase I reaction mixture (66 μl) was overlaid onto the tissue sections, which were then enclosed in a frame. The slides were reacted in an aluminum box at 37°C for 20 min and inactivated at 97°C for 10 min. They were then washed in DEPC-treated water, dehydrated in 99.5% ethanol, and air dried.

Moloney murine leukemia virus (MMLV) reverse transcriptase (10 U/μl; Invitrogen, Carlsbad, CA) was used in a reaction mixture containing 10 mM Tris-HCl (pH 8.3), 50 mM KCl, 5.0 mM $MgCl_2$, 1 μM antisense primer, 1 mM dNTPs, 2 U/μl RNase inhibitor (Takara, Otsu, Japan), and 10 mM dithiothreitol (DTT). The specimens were then overlaid with the mixture, reacted at 42°C for 60 min, washed with distilled water, dehydrated in 99.5% ethanol, and air dried. The subsequent procedures were the same as described for PCR-ISH.

Immunohistochemical staining for detecting HBV proteins. Deparaffinized formaldehyde-fixed sections or fixed frozen liver tissue sections on glass slides were soaked in distilled water, digested with 0.1% pronase (protease P8038 XXIV; Sigma-Aldrich, Tokyo, Japan) for 1 min, and washed with PBS at room temperature. After 30 min of incubation in blocking reagent (1% BSA and 2.5 mM EDTA in PBS) at room temperature, the slides were reacted with 100 μl of anti-HBs and anti-HBc polyclonal antibody solutions for 3 h at room temperature and then overnight at 4°C. The following polyclonal antibodies were used: anti-HBs rabbit polyclonal antibody anti-HBc rabbit polyclonal antibody (Novocastra Laboratories, Newcastle, United Kingdom), or normal rabbit serum diluted in blocking reagent. After the reaction, the slides were washed four times with PBS at room temperature and incubated for 60 min at room temperature in 100 μl anti-rabbit IgG conjugated with peroxidase (Amersham ECL; GE Healthcare, Piscataway, NJ) diluted to 1:100 in blocking reagent. The slides were then washed four times with PBS at room temperature and stained by using 3,3′-diaminobenzidine tetrahydrochloride (DAB) (Vector Labs). Following counterstaining with Mayer's hematoxylin solution, the tissue specimens were dehydrated in 99.5% ethanol and 80% xylene. The slides were sealed by using Bioleit (Oken Shoji, Tokyo, Japan).

RT-PCR–ISH for detecting HCV RNA. HCV RNA was detected by using methods similar to those used for detecting HBV RNA except for the following steps: the DNase I step was omitted, and 1.5 mM $MgCl_2$ was used in the PCR mixture.

Primers and probe sets in RTD-PCR for quantifying HBV DNA, HCV RNA, β-actin DNA, and GAPDH mRNA. The primer sets to quantify the S and X regions of HBV were the same as those used for PCR-ISH. The TaqMan probes for these regions, the primers and probe designed to quantify the 5′-UTR of HCV (33), and those used to quantify β-actin genomic DNA and GAPDH (glyceraldehyde-3-phosphate dehydrogenase) mRNA (internal control) are shown in Table 2. Each PCR comprised 50 cycles (95°C for 30 s, 60°C for 40 s, and 72°C for 30 s) in a real-time PCR system (ABI Prism 7700 sequence detector system; Applied Biosystems).

Amplicor monitor assays. The Amplicor monitor assays were performed as described previously (22, 24, 33, 36).

HE staining. HBV- or HCV-infected deparaffinized formaldehyde-fixed sections or fixed frozen liver tissue sections were stained with hematoxylin and eosin (HE).

LCM of liver tissue. A frozen liver tissue sample was sectioned by using a cryostat and fixed in acetone, followed by HE staining. Laser capture microdissection (LCM) was performed by using an LM 200 system (Olympus, Tokyo, Japan) as described previously (6, 11). This procedure produced approximately 30 hepatocytes from each of three areas (perivenular, intermediate, and periportal) in the section. Total RNA was extracted from the LCM samples, and HCV RNA and GAPDH mRNA were quantified by RTD-PCR.

TABLE 2. Primers and probes for PCR-ISH and RT-PCR

Technique	Virus or protein (region)	Primer or probe		
		Type	Description, nucleotides	Sequence
PCR-ISH	HBV (HBs)	Primer	Forward (HB-166-S21), 166–186	5′-CACATCAGGATTCCTAGGACC-3′
			Reverse (HB-344-R20), 344–325	5′-AGGTTGGTGAGTGATTGGAG-3′
		Probe	(HB-242-S45D), 242–286	5′-(DIG)-CAGAGTCTAGACTCGTGGTGGACTTCTCTCAATTTTCTAGGGGGA-(DIG)n-3′
	HBV (HBx)	Primer	Forward (HB-1584-S21), 1584–1604	5′-CTTCGCTTCACCTCTGCACGT-3′
			Reverse (HB-1744-R23), 1744–1722	5′-CCCAACTCCTCCCAGTCCTTAAA-3′
		Probe	(HB-1705-R45D), 1705–1661	5′-(DIG)-TATGCCTCAAGGTCGGTCGTTGACATTGCTGAGAGTCCAAGAGTC-(DIG)n-3′
RT-PCR–ISH	HCV (5′-UTR)	Primer	Forward (R6-129-S19), 129–147	5′-CCGGGAGAGCCATAGTGGT-3′
			Reverse (R6-290-R19), 290–272	5′-AGTACCACAAGGCCTTTCG-3′
		Probe	(R6-225-S45D), 225–269	5′-(DIG)-ATTTGGGCGTGCCCCCGCGAGACTGCTAGCCGAGTAGTGTTGGGT-(DIG)n-3′
TaqMan	HBV (S)	Probe	Forward (HB-242-S26FT), 242–267	5′-CAGAGTCTAGACTCGTGGTGGACTTC-3′
	HBV (X)	Probe	Forward (HB-1681-S25FT), 1681–1705	5′-TGTCAACGACCGACCTTGAGGCATA-3′
	HCV (5′-UTR)	Primer	Forward (R6-130-S17), 130–146	5′-CGGGAGAGCCATAGTGG-3′
			Reverse (R6-290-R19), 290–272	5′-AGTACCACAAGGCCTTTCG-3′
		Probe	Forward (R6-148-S21FT), 148–168	5′-CTGCGGAACCGGTGAGTACAC-3′
	β-Actin (genomic DNA)	Primer	Forward (β-ACT-1998-S20), 1998–2017	5′-CAGTGTGACATGGTGCATCT-3′
			Reverse (β-ACT-2246-R24), 2246–2223	5′-GTGAGGATCTTCATGAGGTAGTCA-3′
		Probe	Forward (β-ACT-2063-S22FT), 2063–2084	5′-ACGTTGCTATCCAGGCTGTGCT-3′
	GAPDH	Primer	Forward (GAPDH-514-S24), 514–537	5′-TGCACCACCAACTGCTTAGCACCC-3′
			Reverse (GAPDH-837-R24), 837–814	5′-CTTGATGTCATCATATTTGGCAGG-3′
		Probe	Forward (GAPDH-584-S25FT), 584–608	5′-TGACCACAGTCCATGCCATCACTGC-3′

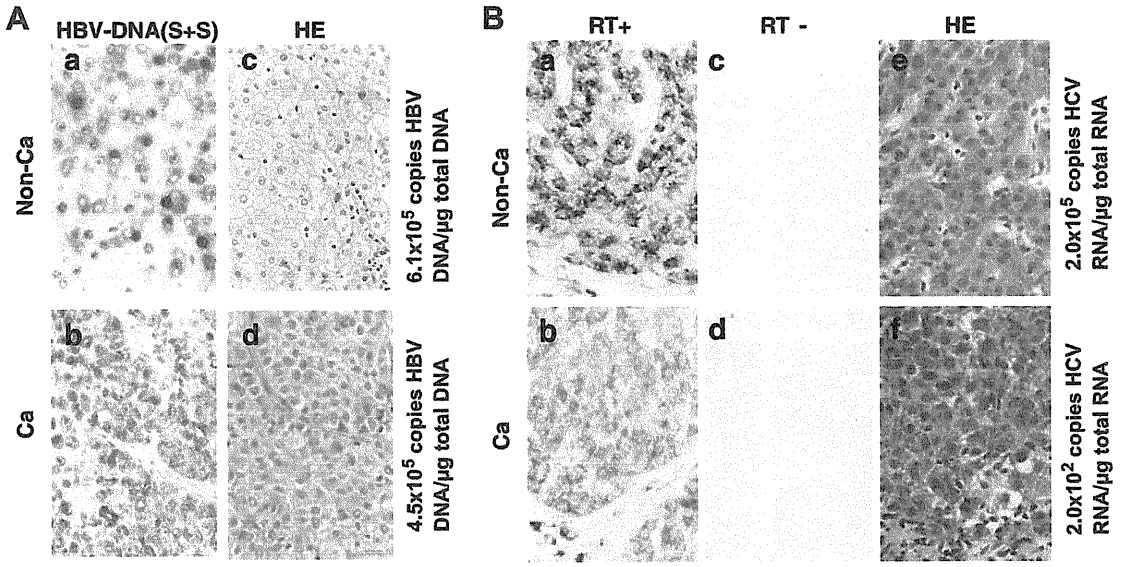

FIG. 1. (A) Panels a and b, HBV DNA detected by PCR-ISH and immunohistochemical staining in noncancerous (Non-Ca) (panel a) and cancerous (Ca) (panel b) liver tissues obtained from a patient infected with HBV. The numbers of PCR cycles were 37 and 42, respectively. Panels c and d, serial sections were stained with HE. Magnification, ×400. S+S, primers and probe targeting the S region of HBV DNA. (B) Panels a and b, HCV RNA detected by RT-PCR–ISH (45 cycles of PCR) in noncancerous (panel a) and cancerous (panel b) tissues obtained from a patient infected with HCV. Panels c and d, no HCV RNA was detected in the RT-negative controls. Panels e and f, serial sections were stained with HE. Magnification, ×400.

RESULTS

Sensitivity and specificity of PCR-ISH versus RTD-PCR for detecting HBV DNA and HCV RNA. PCR-ISH showed positive results for HBV DNA in 10 tissue specimens from eight HBsAg-seropositive patients and two patients whose serum HBV DNA was barely detected by RTD-PCR despite being their HBsAg negative (patients 21 and 22) (Table 1). PCR-ISH yielded negative results for four patients who were negative for serum HBsAg and HCV antibody (patients 23, 24, 28, and 29) and three patients who were negative for serum HBsAg but positive for HCV antibody (patients 9 to 11).

Thirteen of the 14 tissue specimens from the patients with serum HCV antibody had a positive result for HCV RNA by RT-PCR–ISH (sensitivity, 92.9%). In contrast, HCV RNA was not detected by RT-PCR–ISH in four tissue specimens from the patients negative for both HCV antibody and HBsAg (patients 23, 25, 26, and 27) or in the sample from an HBsAg-positive and HCV antibody-negative patient (patient 6).

We performed PCR-ISH and RT-PCR–ISH on the same HBV- or HCV-infected samples from noncancerous and cancerous regions in which we had previously quantitated viral genomic DNA or RNA by RTD-PCR (34). The noncancerous tissue contained 6.1×10^5 copies of HBV DNA/μg total DNA, and the cancerous regions included 4.5×10^5 copies/μg total DNA. Equivalent numbers of cells in the noncancerous and cancerous tissues stained positive for HBV on PCR-ISH (patient 4; Fig. 1A). The PCR-ISH results were consistent with the HBV DNA copy number previously determined by RTD-PCR (34).

Noncancerous tissue from an HCV-positive patient contained 2.0×10^5 copies HCV RNA/μg total RNA, whereas cancerous tissue contained 2.0×10^2 copies/μg total RNA (patient 12; Fig. 1B). HCV RNA was observed by RT-PCR–ISH in hepatocytes of the liver tissue sections from an HCV-infected patient (Fig. 1B). In the noncancerous tissue, an intense hybridization signal was found at the perinuclear sites of almost all the hepatocytes in the section (Fig. 1B, panel a). In contrast, in the cancerous tissue, there was only a weak HCV RNA hybridization signal in the hepatocytes (Fig. 1B, panel b). When the RT step was omitted (control), no HCV RNA was detected in the noncancerous or cancerous tissue sections (Fig. 1B, panels c and d). These results were consistent with the previous quantitation of HCV RNA copy number by RTD-PCR (34).

Detection of HBV DNA by PCR-ISH. HBV DNA was detected by PCR-ISH in the tissue sections obtained from an HBV DNA-seropositive patient. Amplified PCR products were detected by using a probe for either the S or the X region (Fig. 2A, panels a to d) but were not detected by using a heterologous probe (Fig. 2A, panels e and f). Amplification of either the S or the X region of HBV DNA gave the same pattern of hybridization (Fig. 2A, panels a to d). HBV DNA was detected by PCR-ISH in almost all hepatocytes (Fig. 2A, panels a to d) and was very obvious even under low magnification (Fig. 2A, panels a and c). An intense hybridization signal was observed predominantly at the perinuclear site under high magnification (Fig. 2A, panels b and d). In contrast, HBV DNA was not detected by using HBs- and HBx-matched primer and probe combinations in sections obtained from an HBV DNA-seronegative patient (data not shown). DNA fragments amplified by using the S and X region primer sets were 179 bp and 161 bp, respectively (Fig. 2B). Sections from an HBV DNA-seronegative patient were negative in the PCR analysis (data not shown).

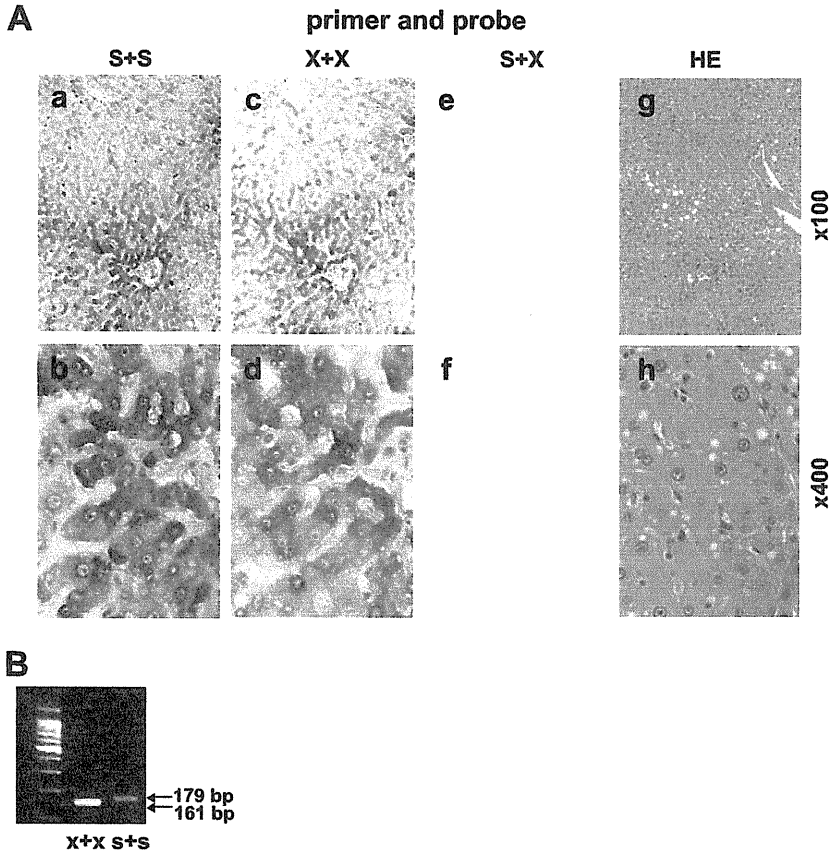

FIG. 2. (A) Panels a to f, HBV DNA detected in liver tissue sections from a patient with chronic hepatitis B by PCR-ISH (42 cycles of PCR). Panels g and h, serial sections were stained with HE. Magnifications, ×100 (panels a, c, e, and g) and ×400 (b, d, f, and h). S+S, primers and probe targeting the S region; X+X, primers and probe targeting the X region; S+X, primers and probe targeting the S and X regions, respectively. (B) Amplified DNA fragments in the PCR mixture of the section in panel A visualized by 3% agarose gel electrophoresis. The PCR product of the X region was 161 bp, and that of the S region was 179 bp.

Localization of HBV DNA, HBV RNA, HBsAg, and HBcAg in liver tissue. HBV DNA, HBV RNA, HBsAg, and HBcAg were detected by PCR-ISH, RT-PCR–ISH, and immunohistochemical staining of serial sections from an HBV-infected patient (patient 5; Fig. 3A, panels a to h). HBV DNA was detected in almost all the hepatocytes by PCR-ISH, although there was wide variation in the hybridization signal intensity between different areas of the section (Fig. 3A, panels a and b). The staining pattern of HBV RNA was similar to that of HBV DNA (Fig. 3A, panels c and d). Intracytoplasmic and intranuclear staining for HBsAg and HBcAg, respectively, was found in some hepatocytes (Fig. 3A, panels f and h). PCR and RT-PCR results were confirmed by gel electrophoresis of the amplified products in the supernatant from the tissue section (Fig. 3B, panels a and b).

Detection of HCV RNA by RT-PCR–ISH. HCV RNA could be detected by RT-PCR–ISH in almost all the hepatocytes in the liver sections obtained from an HCV RNA-seropositive patient (Fig. 4A, panels a and b). Under high magnification, a strong HCV RNA signal was detected in the perinuclear area (Fig. 4A, panel b). A negative-control test (no RT) did not detect any HCV RNA (Fig. 4A, panels c and d). The expected 162-bp DNA fragment amplified by RT-PCR in the supernatant from the tissue section was detected (Fig. 4B, lane 2). In contrast, HCV RNA was not detected in the liver section obtained from an HCV RNA-seronegative patient, regardless of whether RT was used (data not shown).

Isolation of HCV RNA in hepatocytes by LCM. Hepatocyte groups were captured from the perivenular, intermediate, and periportal areas by LCM (Fig. 4C, panel a). HCV RNA was quantified by RTD-PCR in approximately 30 hepatocytes captured by LCM and normalized against the picogram weight of GAPDH mRNA (Fig. 4C, panels b to d); the HCV RNA levels were equivalent in all three regions (Fig. 4C, panel d).

Detection of HCV RNA in the epithelium of the large bile duct. HCV RNA was detected by RT-PCR–ISH in the epithelium of the large bile duct, which was surrounded by dense fibrous and elastic tissue (Fig. 4D, panels a and b). In contrast, no HCV RNA was detected in the epithelium of the small bile duct. Further, HCV RNA was not detected in the portal vein or its branches (Fig. 4D, panel a).

Detection of HBV DNA and HCV RNA in noncancerous and cancerous liver tissue sections obtained from a patient with HBV and HCV coinfection. Figure 5 shows the results for HBV DNA and HCV RNA in liver samples from a patient with HCC having HCV and HBV coinfection. The amounts of serum HBV DNA and HCV RNA were 39 copies/ml and 5×10^7 copies/ml, respectively (patient 21) (34). In the noncancerous

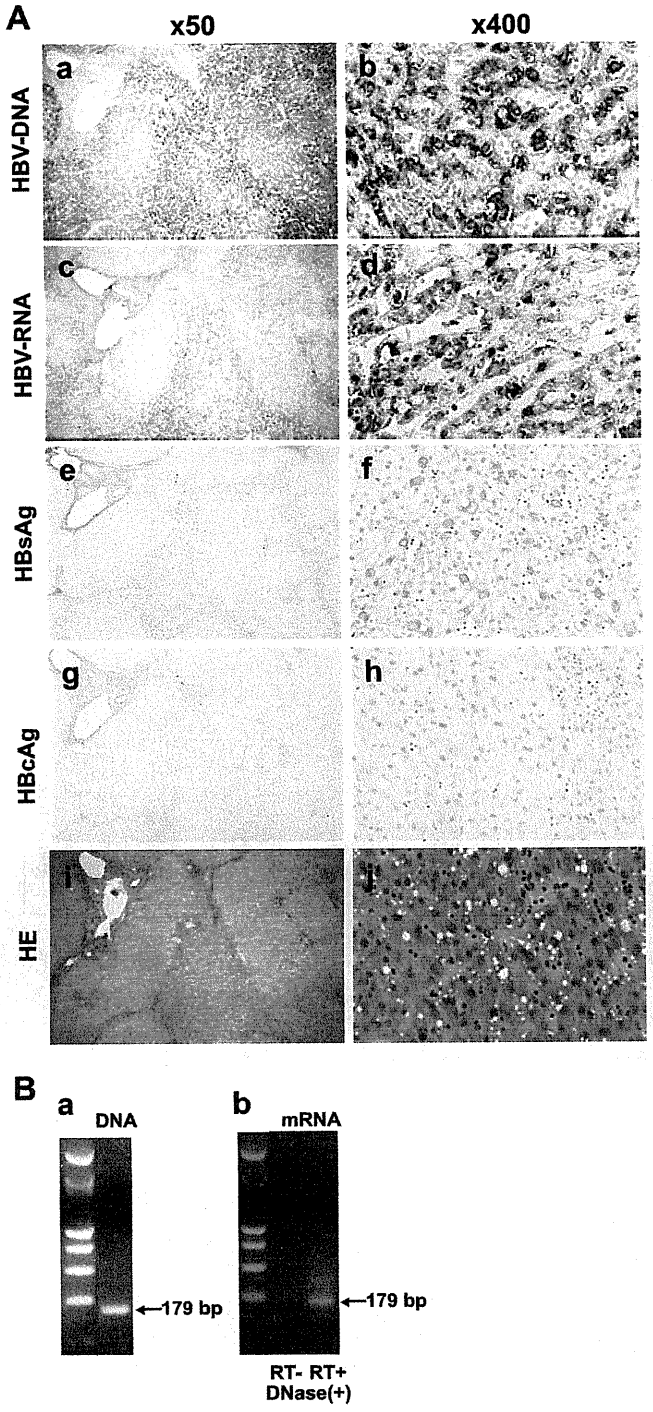

FIG. 3. (A) Panels a to h, HBV DNA, HBV RNA, HBsAg, and HBcAg detected in OCT-embedded frozen liver tissue from a patient with chronic hepatitis B by PCR-ISH (panels a and b), RT-PCR–ISH (panels c and d), and immunohistochemical staining (panels e to h). Panels i and j, HE staining of serial sections. The primers and probe targeted the S region to detect HBV DNA and HBV RNA. Antibodies to the envelope and core proteins were used to detect HBsAg and HbcAg, respectively. Magnifications, ×50 (panels a, c, e, g, and i) and ×400 (panels b, d, f, h, and j). The number of PCR cycles was 42. (B) Amplified DNA fragments in the PCR mixture of the section in panel A. Panel a, the DNA fragments amplified by 42 cycles of PCR were visualized by 3% agarose gel electrophoresis. Panel b, RT-PCR after DNase I treatment (3 U/μl) and negative controls (no RT).

tissue from the patient with HBV and HCV coinfection, there was an intense hybridization signal for HCV RNA on RT-PCR–ISH in almost all the hepatocytes (Fig. 5A, panel b). There was also a positive but weak RT-PCR–ISH signal for HCV RNA in the tumor hepatocytes (Fig. 5B, panel b). Few hepatocytes in the cancerous tissue were positive for HBV DNA by PCR-ISH (Fig. 5B, panel a), and no HBV DNA hybridization signal was detected in the noncancerous tissue (Fig. 5A, panel a).

DISCUSSION

The standard assay for detecting replication of HBV and HCV in tissue is ISH, but results are often inconsistent and sometimes difficult to reproduce. The specificity of ISH is high but its sensitivity low, and it is difficult to detect low copy numbers of the HBV or HCV genome in tissue. PCR technology has been adapted to *in situ* amplification of viral genomes or their replicative intermediates in liver tissue sections, but sensitivity and specificity remain major challenges to the application of this approach (13, 18, 23, 25, 26, 30, 31). Here, we describe the use of a novel, highly specific and sensitive PCR-ISH method to determine the distribution and localization of HBV DNA, HBV RNA, and HCV RNA in both normal and cancerous liver tissues.

PCR-ISH is the most sensitive technology currently available for the detection of viral genomes, but a major potential limitation of this approach is the low specificity. We were able to improve the specificity of PCR-ISH by careful optimization of certain steps. PCR was performed using sets of antisense and sense primers that were complementary to the sequences located in the S and X regions of HBV and the 5′-UTR upstream of the core region of HCV. We added PCR templates to the PCR mixture and then added the PCR mixture to the HBV- or HCV-negative tissue sections. The slides were placed in the GeneAmp *in situ* PCR system 1000 unit, and PCR-ISH was performed as described in Materials and Methods. Following these results, we selected the primer and probe set that did not stain the HBV- or HCV-negative tissue sections by PCR-ISH. Second, the type and concentration of protease and the treatment time were adjusted to optimize permeabilization of membranes and release of protein-nucleic acid cross-linking while avoiding overdigestion. Third, to improve the specificity for detecting viral genomes, we limited the number of PCR cycles and fixed the liver tissue sections in 4% paraformaldehyde immediately after PCR amplification. This step is essential to avoid diffusion of PCR products into neighboring cells, a phenomenon known as the diffusion artifact. Limiting the number of PCR cycles was also important for eliminating the background staining, as too many cycles resulted in high background staining and loss of tissue morphology. Fourth, we added a DIG-dUTP tail at the 3′ ends of the probes for PCR-ISH and RT-PCR–ISH. These 45-mer probes were optimized to improve their sensitivity without impairing the specificity.

HBV DNA was detected by PCR-ISH in a large number of hepatocytes in tissue sections from an HBV DNA-seropositive patient (Fig. 1A, panel a). HBV DNA was also observed by PCR-ISH in tumor hepatocytes in a section of cancerous tissue from the same patient (Fig. 1A, panel b). As shown in Fig. 2A,

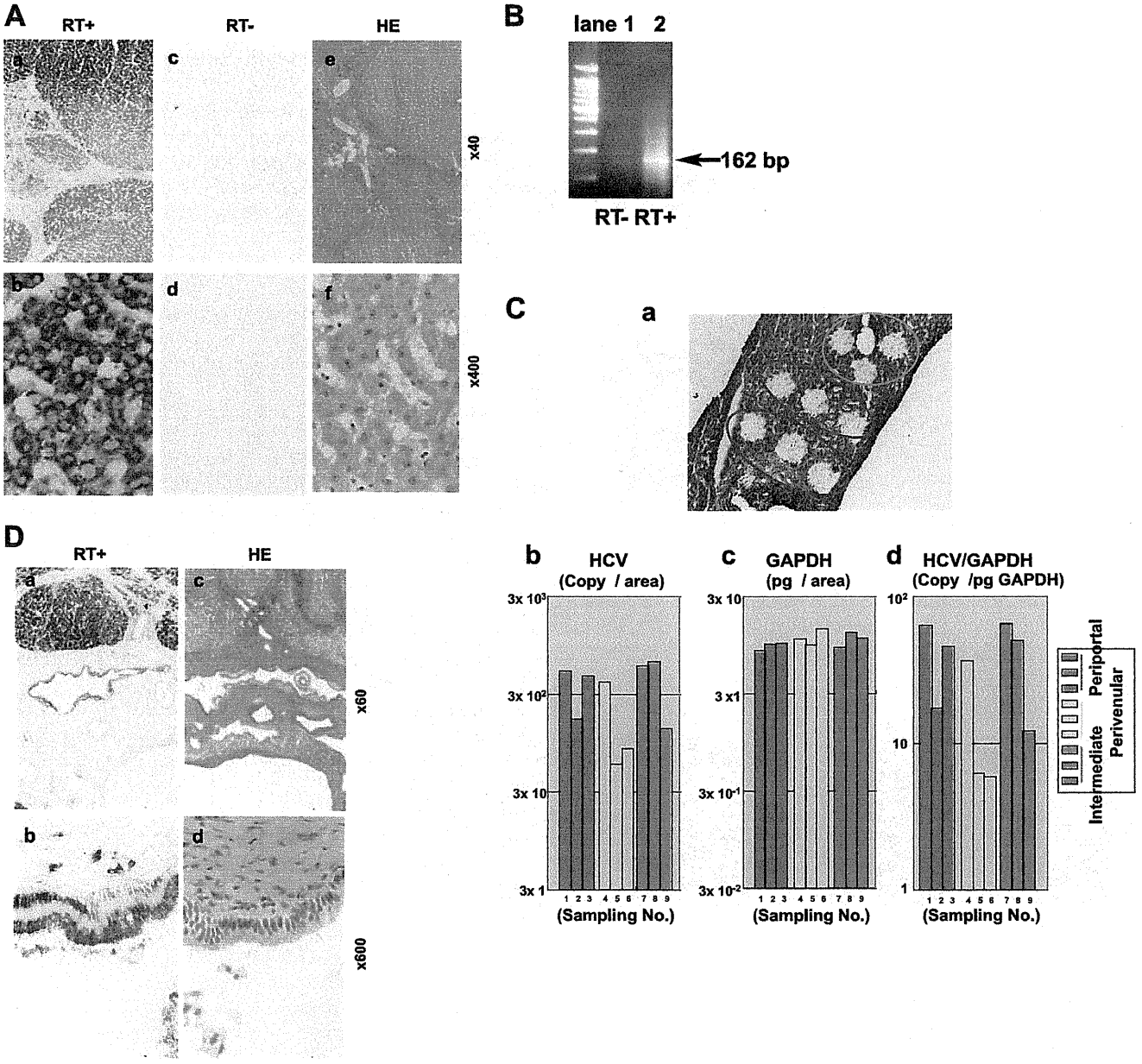

FIG. 4. (A) Panels a and b, HCV RNA detected in liver tissue samples from a patient with chronic hepatitis C by RT-PCR–ISH. Panels c and d, HCV RNA was not detected in a negative control (no RT). The number of PCR cycles was 45. Panels e and f, serial sections were stained with HE. Magnifications, ×40 (panels a, c, and e) and ×400 (panels b, d, and f). (B) DNA fragments in the PCR mixture of the section in panel A were amplified with the RT step and detected by 3% agarose gel electrophoresis. Amplification without the RT step resulted in no detection of DNA fragments. (C) Panel a, after LCM of nine areas, sections of liver tissue obtained from a patient with chronic hepatitis C were stained with HE. Panels b and c, HCV RNA and GAPDH mRNA in each of the areas were quantified by RTD-PCR, and the results are expressed as copy number per LCM area. Panel d, the copy number of HCV RNA was corrected by using the picogram weight of GAPDH. (D) Panels a and b, HCV RNA detected in the epithelium of the large bile duct by RT-PCR–ISH. The number of PCR cycles was 45. Panels c and d, serial sections were stained with HE. Magnifications, ×60 (a and c) and ×600 (b and d).

we obtained clear and reproducible patterns of distribution or localization of the viral genomes in the tissue sections. The visual patterns of HBV DNA distribution were similar, irrespective of the primer sets and probes (Fig. 2A, panels a to d). These data indicate that our technique is highly specific and reproducible for the detection of HBV DNA.

The staining pattern of HBV RNA was similar to that of HBV DNA (Fig. 3A, panels c and d). HBV DNA was also observed by PCR–ISH in tumor hepatocytes in a section of cancerous tissue from an HBV DNA-seropositive patient (Fig. 1A, panel b), but neither HBsAg nor HBcAg was detected in this section (data not shown). As shown in Fig. 3, the intensity of HBV DNA by PCR-ISH was almost the same as that of HBV RNA by RT-PCR–ISH but did not coincide with the

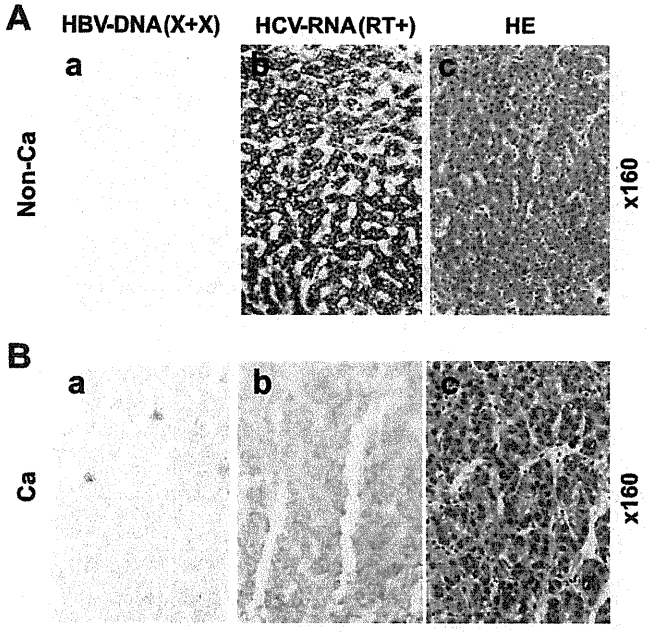

FIG. 5. Panels a and b, HBV DNA (panels a) and HCV RNA (panels b) in noncancerous (non-Ca) (A) and cancerous (Ca) (B) liver tissue obtained from a patient coinfected with HBV and HCV were detected by PCR-ISH (55 cycles of PCR) and RT-PCR–ISH (45 cycles of PCR), respectively. Panels c, serial sections were stained with HE. Magnification, ×160.

intensity of HBV protein expression. HBV has four overlapping open reading frames regulated by two enhancer elements and four promoters (14).

We had reported previously that HCV RNA and HCV core protein levels are relatively stable irrespective of fibrosis (33, 35). In the present study, HCV RNA was detected in almost all hepatocytes in all sections. Furthermore, we emphasize the similar staining pattern of almost all hepatocytes at the cellular level. HCV RNA was detected in the cytoplasm but not in the nucleus. The detection of an intense signal at the perinuclear site may reflect the replication process of HCV (10). HCV RNA was also detected in the epithelium of the large bile duct but not in the endothelial cells, portal tracts, or sinusoidal lymphocytes, which is consistent with the results of previous studies (5, 8). Thus, the epithelium of the large bile duct, but not that of the small duct, can support HCV replication.

We confirmed the specificity for detecting the HCV RNA copy number by quantification in a small area of an LCM section (Fig. 4C); similar amounts of HCV RNA were detected in each area. The detection of HCV RNA in each area by LCM and RTD-PCR excluded the possibility of diffusion of the PCR product by RT-PCR–ISH.

Recent molecular biological techniques have demonstrated low-level HBV viremia in some patients with chronic hepatitis C who were negative for all serological HBV markers. In these cases, HBV DNA not only is integrated in the human chromosomes but also replicates in hepatocytes (34). In the previous study, we measured the levels of HBV DNA and HCV RNA using RTD-PCR with singly infected or coinfected noncancerous and cancerous liver tissues (34). In the case of coinfection, HCV replication was dominant in the noncancerous tissue whereas HBV replication was dominant in the cancerous tissue. Some studies have shown that HCV inhibits HBV gene expression and replication (7, 15).

Using this novel, highly specific and sensitive PCR-ISH method, we could visualize the tissue staining patterns of HBV and HCV, which were consistent with those seen by RTD-PCR. This revealed the novel finding that almost all hepatocytes are infected with HBV or HCV in patients with chronic liver disease, suggesting that the viruses spread throughout the liver in the chronic stage. However, further study with a large number of samples from each stage of infection is needed to clarify the mechanism of persistent infection via our assay method.

ACKNOWLEDGMENTS

We are grateful to Yuichi Hirata of the Tokyo Metropolitan Institute of Medical Science and Kyoko Kohara of Kumamoto University for their critical comments and helpful discussions.

This study was supported by grants from the Ministry of Education, Culture, Sports, Science and Technology of Japan, the Program for Promotion of Fundamental Studies in Health Sciences of the Pharmaceuticals and Medical Devices Agency of Japan, and the Ministry of Health, Labor and Welfare of Japan.

REFERENCES

1. **Abe, A., K. Inoue, T. Tanaka, J. Kato, N. Kajiyama, R. Kawaguchi, S. Tanaka, M. Yoshiba, and M. Kohara.** 1999. Quantitation of hepatitis B virus genomic DNA by real-time detection PCR. J. Clin. Microbiol. **37**:2899–2903.
2. **Beasley, R. P., L. Y. Hwang, C. C. Lin, and C. S. Chien.** 1981. Hepatocellular carcinoma and hepatitis B virus. A prospective study of 22 707 men in Taiwan. Lancet **ii**:1129–1133.
3. **Bedossa, P., and T. Poynard.** 1996. An algorithm for the grading of activity in chronic hepatitis C. The METAVIR Cooperative Study Group. Hepatology **24**:289–293.
4. **Benvegnù, L., G. Fattovich, F. Noventa, F. Tremolada, L. Chemello, A. Cecchetto, and A. Alberti.** 1994. Concurrent hepatitis B and C virus infection and risk of hepatocellular carcinoma in cirrhosis. A prospective study. Cancer **74**:2442–2448.
5. **Boletis, J. N., J. K. Delladetsima, F. Makris, H. Theodoropoulou, S. Vgenopoulou, A. Kostakis, and A. Hatzakis.** 2000. Cholestatic syndromes in renal transplant recipients with HCV infection. Transpl. Int. **13**(Suppl. 1):S375–S379.
6. **Bonner, R. F., M. Emmert-Buck, K. Cole, T. Pohida, R. Chuaqui, S. Goldstein, and L. A. Liotta.** 1997. Laser capture microdissection: molecular analysis of tissue. Science **278**:1481–1483.
7. **Chen, S. Y., C. F. Kao, C. M. Chen, C. M. Shih, M. J. Hsu, C. H. Chao, S. H. Wang, L. R. You, and Y. H. Lee.** 2003. Mechanisms for inhibition of hepatitis B virus gene expression and replication by hepatitis C virus core protein. J. Biol. Chem. **278**:591–607.
8. **Delladetsima, J. K., F. Makris, M. Psichogiou, A. Kostakis, A. Hatzakis, and J. N. Boletis.** 2001. Cholestatic syndrome with bile duct damage and loss in renal transplant recipients with HCV infection. Liver **21**:81–88.
9. **Di Bisceglie, A. M., S. E. Order, J. L. Klein, J. G. Waggoner, M. H. Sjogren, G. Kuo, M. Houghton, Q. L. Choo, and J. H. Hoofnagle.** 1991. The role of chronic viral hepatitis in hepatocellular carcinoma in the United States. Am. J. Gastroenterol. **86**:335–338.
10. **El-Hage, N., and G. Luo.** 2003. Replication of hepatitis C virus RNA occurs in a membrane-bound replication complex containing nonstructural viral proteins and RNA. J. Gen. Virol. **84**:2761–2769.
11. **Emmert-Buck, M. R., R. F. Bonner, P. D. Smith, R. F. Chuaqui, Z. Zhuang, S. R. Goldstein, R. A. Weiss, and L. A. Liotta.** 1996. Laser capture microdissection. Science **274**:998–1001.
12. **Fattovich, G.** 2003. Natural history and prognosis of hepatitis B. Semin. Liver Dis. **23**:47–58.
13. **Fragulidis, G. P., R. E. Cirocco, D. Weppler, M. Berho, G. Gillian, M. Markou, A. Viciana, V. Esquenazi, J. R. Nery, J. Miller, K. R. Reddy, and A. G. Tzakis.** 1998. In situ enzymatic oligonucleotide amplification of hepatitis C virus-RNA in liver biopsy specimens (reverse transcriptase in situ polymerase chain reaction) after orthotopic liver transplantation for hepatitis C-related liver disease. Transplantation **66**:1472–1476.
14. **Ganem, D., and A. M. Prince.** 2004. Hepatitis B virus infection—natural history and clinical consequences. N. Engl. J. Med. **350**:1118–1129.
15. **Guo, H., T. Zhou, D. Jiang, A. Cuconati, G.-H. Xiao, T. M. Block, and J.-T. Guo.** 2007. Regulation of hepatitis B virus replication by the phosphatidylinositol 3-kinase-akt signal transduction pathway. J. Virol. **81**:10072–10080.

16. **Holland, P. V., and H. J. Alter.** 1975. The clinical significance of hepatitis B virus antigens and antibodies. Med. Clin. North Am. **59:**849–855.
17. **Kiyosawa, K., T. Sodeyama, E. Tanaka, Y. Gibo, K. Yoshizawa, Y. Nakano, S. Furuta, Y. Akahane, K. Nishioka, R. H. Purcell, et al.** 1990. Interrelationship of blood transfusion, non-A, non-B hepatitis and hepatocellular carcinoma: analysis by detection of antibody to hepatitis C virus. Hepatology **12:**671–675.
18. **Komminoth, P., A. A. Long, R. Ray, and H. J. Wolfe.** 1992. In situ polymerase chain reaction detection of viral DNA, single-copy genes, and gene rearrangements in cell suspensions and cytospins. Diagn. Mol. Pathol. **1:**85–97.
19. **Kuo, G., Q. L. Choo, H. J. Alter, G. L. Gitnick, A. G. Redeker, R. H. Purcell, T. Miyamura, J. L. Dienstag, M. J. Alter, C. E. Stevens, et al.** 1989. An assay for circulating antibodies to a major etiologic virus of human non-A, non-B hepatitis. Science **244:**362–364.
20. **Large, M. K., D. J. Kittlesen, and Y. S. Hahn.** 1999. Suppression of host immune response by the core protein of hepatitis C virus: possible implications for hepatitis C virus persistence. J. Immunol. **162:**931–938.
21. **Leone, N., and M. Rizzetto.** 2005. Natural history of hepatitis C virus infection: from chronic hepatitis to cirrhosis, to hepatocellular carcinoma. Minerva Gastroenterol. Dietol. **51:**31–46.
22. **Navas, S., and V. Carreno.** 1995. Semiquantification by Amplicor assay of hepatitis C virus genome during therapy. J. Hepatol. **22:**115–117.
23. **Negro, F.** 1998. Detection of hepatitis C virus RNA in liver tissue: an overview. Ital. J. Gastroenterol. Hepatol. **30:**205–210.
24. **Nolte, F. S., C. Thurmond, and M. W. Fried.** 1995. Preclinical evaluation of AMPLICOR hepatitis C virus test for detection of hepatitis C virus RNA. J. Clin. Microbiol. **33:**1775–1778.
25. **Nuovo, G. J., F. Gallery, P. MacConnell, J. Becker, and W. Bloch.** 1991. An improved technique for the in situ detection of DNA after polymerase chain reaction amplification. Am. J. Pathol. **139:**1239–1244.
26. **Nuovo, G. J., P. MacConnell, A. Forde, and P. Delvenne.** 1991. Detection of human papillomavirus DNA in formalin-fixed tissues by in situ hybridization after amplification by polymerase chain reaction. Am. J. Pathol. **139:**847–854.
27. **Sansonno, D., V. Cornacchiulo, V. Racanelli, and F. Dammacco.** 1997. In situ simultaneous detection of hepatitis C virus RNA and hepatitis C virus-related antigens in hepatocellular carcinoma. Cancer **80:**22–33.
28. **Schluger, L. K., P. A. Sheiner, S. N. Thung, J. Y. Lau, A. Min, D. C. Wolf, I. Fiel, D. Zhang, M. A. Gerber, C. M. Miller, and H. C. Bodenheimer, Jr.** 1996. Severe recurrent cholestatic hepatitis C following orthotopic liver transplantation. Hepatology **23:**971–976.
29. **Seeger, C., and W. S. Mason.** 2000. Hepatitis B virus biology. Microbiol. Mol. Biol. Rev. **64:**51–68.
30. **Shieh, B., S.-E. Lee, Y.-C. Tsai, I.-J. Su, and C. Li.** 1999. Detection of hepatitis B virus genome in hepatocellular carcinoma tissues with PCR-in situ hybridization. J. Virol. Methods **80:**157–167.
31. **Shin, Y. J., S. W. Cho, K. B. Hahm, Y. S. Kim, J. H. Kim, K. H. Park, and S. I. Lee.** 1998. Localization of hepatitis B virus DNA in hepatocellular carcinoma by polymerase chain reaction in situ hybridization. J. Korean Med. Sci. **13:**377–382.
32. **Shiratori, Y., S. Shiina, P. Y. Zhang, E. Ohno, T. Okudaira, D. A. Payawal, S. K. Ono-Nita, M. Imamura, N. Kato, and M. Omata.** 1997. Does dual infection by hepatitis B and C viruses play an important role in the pathogenesis of hepatocellular carcinoma in Japan? Cancer **80:**2060–2067.
33. **Takeuchi, T., A. Katsume, T. Tanaka, A. Abe, K. Inoue, K. Tsukiyama-Kohara, R. Kawaguchi, S. Tanaka, and M. Kohara.** 1999. Real-time detection system for quantification of hepatitis C virus genome. Gastroenterology **116:**636–642.
34. **Tanaka, T., K. Inoue, Y. Hayashi, A. Abe, K. Tsukiyama-Kohara, H. Nuriya, Y. Aoki, R. Kawaguchi, K. Kubota, M. Yoshiba, M. Koike, S. Tanaka, and M. Kohara.** 2004. Virological significance of low-level hepatitis B virus infection in patients with hepatitis C virus associated liver disease. J. Med. Virol. **72:**223–229.
35. **Tanaka, T., J. Y. Lau, M. Mizokami, E. Orito, E. Tanaka, K. Kiyosawa, K. Yasui, Y. Ohta, A. Hasegawa, S. Tanaka, et al.** 1995. Simple fluorescent enzyme immunoassay for detection and quantification of hepatitis C viremia. J. Hepatol. **23:**742–745.
36. **Zeuzem, S., B. Rüster, and W. K. Roth.** 1994. Clinical evaluation of a new polymerase chain reaction assay (Amplicor HCV) for detection of hepatitis C virus. Z Gastroenterol. **32:**342–347.

JOURNAL OF VIRAL HEPATITIS JVH

Journal of Viral Hepatitis, 2010, 17, 859–865 doi:10.1111/j.1365-2893.2009.01253.x

Association between phospholipids and free cholesterol in high-density lipoprotein and the response to hepatitis C treatment in Japanese with genotype 1b

H. Mawatari,[1] M. Yoneda,[1] K. Fujita,[1] Y. Nozaki,[1] Y. Shinohara,[1] H. Sasaki,[2] H. Iida,[1] H. Takahashi,[1] M. Inamori,[1] Y. Abe,[1] N. Kobayashi,[1] K. Kubota,[1] H. Kirikoshi,[1] A. Nakajima[1] and S. Saito[1]

[1]*Gastroenterology Division, Yokohama City University School of Medicine, Fukuura, Kanazawa-ku, Yokohama City, Japan; and* [2]*Skylight Biotech Inc., Sunada, Iijima-aza, Akita, Japan*

Received August 2009; accepted for publication October 2009

SUMMARY. Pegylated interferon and ribavirin combination therapy is the standard treatment for patients with chronic hepatitis C (CHC), but treatment failure can be difficult to predict. We and others have reported a relation between lipid values and sustained viral responses in patients with CHC. However, the relationship between lipid values and treatment failure has not been previously reported. The present study investigated the association between the profiles of phospholipids and free cholesterol (FC), the main constitutive ingredients of the surface of lipoprotein, classified according to particle size and hepatitis C treatment, and determined the usefulness of these parameters for predicting the outcome of treatment. Fifty-five patients with CHC (33 men and 22 women) were included in the study. The serum total cholesterol, triglyceride, phospholipids, and FC levels in the lipoprotein subclasses were determined using high-performance liquid chromatography with gel permeation columns, enabling the lipoproteins to be classified into 13 subclasses according to particle size. According to a univariate analysis, the treatment failure group had a significantly higher serum phospholipid level overall in the high-density lipoprotein (HDL) and medium HDL fractions as well as a higher serum FC level in the HDL fraction and all HDL subclass fractions compared with the corresponding values in the non-nonvirological response group. Higher serum phospholipid and FC concentrations in the HDL subclasses were predictive of a failure to respond in patients with genotype 1b.

Keywords: free cholesterol, hepatitis C virus, high-performance liquid chromatography, interferon, nonvirological responses, phospholipid.

INTRODUCTION

About 200 million people worldwide are reportedly infected with hepatitis C virus (HCV), making HCV infection a major public health problem [1,2]. The virus cannot be eradicated in the majority of patients infected with HCV, and in some cases, HCV infection progresses to liver failure and hepatocellular carcinoma [3,4]. The distribution of major HCV genotypes varies according to geographical region, with genotype 1b being the most common in Japan. The HCV genotype has been identified as an important predictor of treatment efficacy, and no more than approximately 50% of patients with genotype 1b achieve a sustained viral response (SVR) after combined treatment with pegylated interferon plus ribavirin (PEG-IFN-RBV) [5,6]. Factors that may influence disease progression and response to therapy have been extensively investigated. These variables include age at the time of infection, sex, alcohol consumption, duration of infection, race, HCV genotype, viral load, and fibrotic stage. Modifications in lipid metabolism during the course of chronic hepatitis C (CHC) have also been studied [7–9].

Previously, we used computer-assisted high-performance liquid chromatography (HPLC) followed by the mathematical examination of chromatograms to examine the relation of cholesterol and triglyceride (TG) levels in lipoprotein subclasses among 44 patients with HCV infection [10]. This innovative method enables the serum lipid levels to be determined in each lipoprotein subfraction according to particle size [11–13]. We reported that higher serum

Abbreviations: CE, cholesteryl ester; CHC, chronic hepatitis C; FC, free cholesterol; HCV, hepatitis C virus; HDL, high-density lipoprotein; NVRs, nonvirological responses; PL, phospholipid; SVR, sustained viral response; VLDL, very low-density lipoprotein.

Correspondence: Satoru Saito, Gastroenterology Division, Yokohama City University School of Medicine, 3-9, Fukuura, Kanazawa-ku, Yokohama City 236-0004, Japan.
E-mail: ssai1423@yokohama-cu.ac.jp

cholesterol and TG concentrations in the lipoprotein subfractions were predictive of an SVR to therapy for infection with HCV (genotype 1b). No significant difference in the levels of TG and cholesterol in lipoprotein subfraction was observed between nonvirological responses (NVRs) to hepatitis C treatment and non-NVR. Most of the cholesterol and TG molecules are main constitutive ingredients of the inside of lipoprotein. The surface of lipoprotein contains phospholipid (PL), free cholesterol (FC), and apolipoproteins. In this study, we used computer-assisted HPLC to examine the levels of PL and FC, the main constitutive ingredients of the surface of lipoprotein. The aim of this study was to investigate the association between the levels of PL and FC in lipoprotein subclasses and hepatitis C treatment and to determine the clinical usefulness of the lipoprotein profiles for predicting a NVR to therapy for CHC prior to the start of interferon treatment.

PATIENTS AND METHODS

A total of 55 CHC Japanese patients with genotype 1b (mean ± standard deviation [SD] for age, 54.3 ± 12.4 years; age range, 25–72 years) were selected from among 131 consecutive patients who had received PEG-IFN-RBV combination therapy between April 2005 and October 2007 at Yokohama City University Hospital. The patients were selected based on the following criteria: (i) infection with HCV genotype 1b only; (ii) a high viral load (over 100 KIU/mL) according to a quantitative analysis [polymerase chain reaction (PCR)] of HCV-RNA (Cobas Amplicor HCV monitor v. 2.0, using the 10-fold dilution method; Roche K.K., Tokyo, Japan) performed within the 3 months preceding treatment; (iii) no severe fibrosis or cirrhosis visible at the time of liver biopsy [14]; (iv) no diabetes mellitus or renal disease; (v) no treatment with any lipid-lowering medication; (vi) no other forms of hepatitis, such as hemochromatosis, Wilson's disease, primary biliary cirrhosis, alcoholic liver disease, or autoimmune liver disease; (vii) no pregnant or lactating women; and (viii) an SVR assessed at least 24 weeks after the cessation of combined treatment. Each patient signed a consent form for the study protocol that had been approved by the Ethics Committee of Yokohama City University Hospital. In all the patients, plasma samples collected within 1 month before the start of treatment were available and were used to determine the fasting lipoprotein levels.

The PEG-IFNa-2b dose was adjusted according to body weight (60 μg for >35 and ≤45 kg, 80 μg for >45 and ≤60 kg, 100 μg for >60 and ≤75 kg, 120 μg for >75 and ≤90 kg, and 150 μg for >90 and ≤120 kg). The RBV dose was also adjusted according to body weight (600 mg for ≤60 kg, 800 mg for >60 and ≤80 kg, and 1000 mg for >80 kg). The patients received PEG-IFNa-2b at a median dose of 1.44 μg/kg (range, 0.91–1.72 μg/kg) subcutaneously each week and RBV orally at a median dose of 11.5 mg/kg (range, 8.0–14.0 mg/kg) daily for 48 weeks.

Patients who did not become negative for HCV-RNA during treatment were regarded as having an NVR. The patients were divided into NVR and non-NVR groups. The non-NVR group was composed of patients who relapsed and sustained negativity after the completion of treatment.

An HPLC system with two tandem gel permeation columns (Skylight Biotech, Inc., Akita, Japan) was used to evaluate the size distribution of the plasma lipoprotein particles [12,13,15]. Samples were diluted 20 times and analysed at a flow rate of 350 μL/min by monitoring the concentrations of choline-PL, total cholesterol, and TG, with an absorbance set at 585 nm for choline-PL and at 550 nm for cholesterol and TG. The particle sizes for individual subfractions were previously determined as 44.5–64 nm [large very low-density lipoprotein (VLDL)], 36.8 nm

Table 1 Basic clinical characteristics and major lipid profiles

Parameter	Total (n = 55)	NVR (n = 12)	Non-NVR (n = 43)	P
Basic clinical characteristics				
Age (years)	54.3 ± 12.4	56.8 ± 10.4	53.7 ± 13.2	0.461
Male sex (%)	60.0 ± 49.4	58.3 ± 51.5	60.5 ± 49.5	0.896
Body mass index (kg/m^2)	22.9 ± 3.1	23.9 ± 2.7	22.6 ± 3.2	0.232
Serum aspartate aminotransferase (IU/L)	57.1 ± 34.9	57.9 ± 28.7	56.9 ± 36.8	0.932
Serum alanine aminotransferase (IU/L)	73.4 ± 47.9	68.1 ± 36.9	74.9 ± 50.9	0.668
Hepatitis C virus -RNA load (KIU/mL)	1993 ± 1426	1916 ± 1454	2017 ± 1435	0.834
Major lipids				
Total cholesterol (mg/dL)	166.1 ± 30.1	163.2 ± 39.2	166.9 ± 27.5	0.708
High-density lipoprotein cholesterol (mg/dL)	50.9 ± 15.2	57.4 ± 22.5	49.0 ± 12.2	0.090
Low-density lipoprotein cholesterol (mg/dL)	32.9 ± 21.0	78.6 ± 22.5	84.0 ± 20.0	0.433
Triglycerides (mg/dL)	99.2 ± 29.4	97.4 ± 27.4	99.7 ± 30.2	0.809

The values are shown as the mean ± standard deviation (SD). NVR, nonvirological response to pegylated interferon plus ribavirin combination therapy.

(medium VLDL), 31.3 nm (small VLDL), 28.6 nm [large low-density lipoprotein (LDL)], 25.5 nm (medium LDL), 23 nm (small LDL), 16.7–20.7 nm (very small LDL), 13.5–15 nm [very large high-density lipoprotein (HDL)], 12.1 nm (large HDL), 10.9 nm (medium HDL), 9.8 nm (small HDL), and 7.6–8.8 nm (very small HDL) [12].

Data are expressed as the mean ± SD, unless indicated otherwise. The statistical analysis was conducted using SPSS 12.0 (SPSS, Chicago, IL, USA). For univariate comparisons between the patient groups, the *t*-test or Mann–Whitney's *U* test was used, where appropriate. $P < 0.05$ was considered significant.

RESULTS

The clinical characteristics and serum concentrations of the major lipoproteins for the 55 patients included in this study are shown in Table 1. The NVR group contained 12 patients (21.8%). No significant differences in age, sex, body mass index, serum aspartate aminotransferase, serum alanine aminotransferase, HCV-RNA load, total cholesterol, HDL-cholesterol, LDL-cholesterol, or TGs were observed between the SVR and non-SVR groups.

The serum PL concentrations in each of the lipoprotein subclasses are shown in Fig. 1b and Table 2. The NVR group exhibited significantly higher medium HDL-PL (31.6 ± 7.6 *vs* 27.0 ± 5.6 mg/dL, $P = 0.025$), total HDL-PL (137.9 ± 38.3 *vs* 111.7 ± 24.6 mg/dL, $P = 0.006$), and total PL (244.5 ± 54.7 *vs* 212.0 ± 31.1 mg/dL, $P = 0.010$) values than the non-NVR group.

The serum FC concentrations in each of the lipoprotein subclasses are shown in Fig. 1a and Table 2. The NVR group had significantly higher serum FC levels in the total HDL and all HDL subclasses.

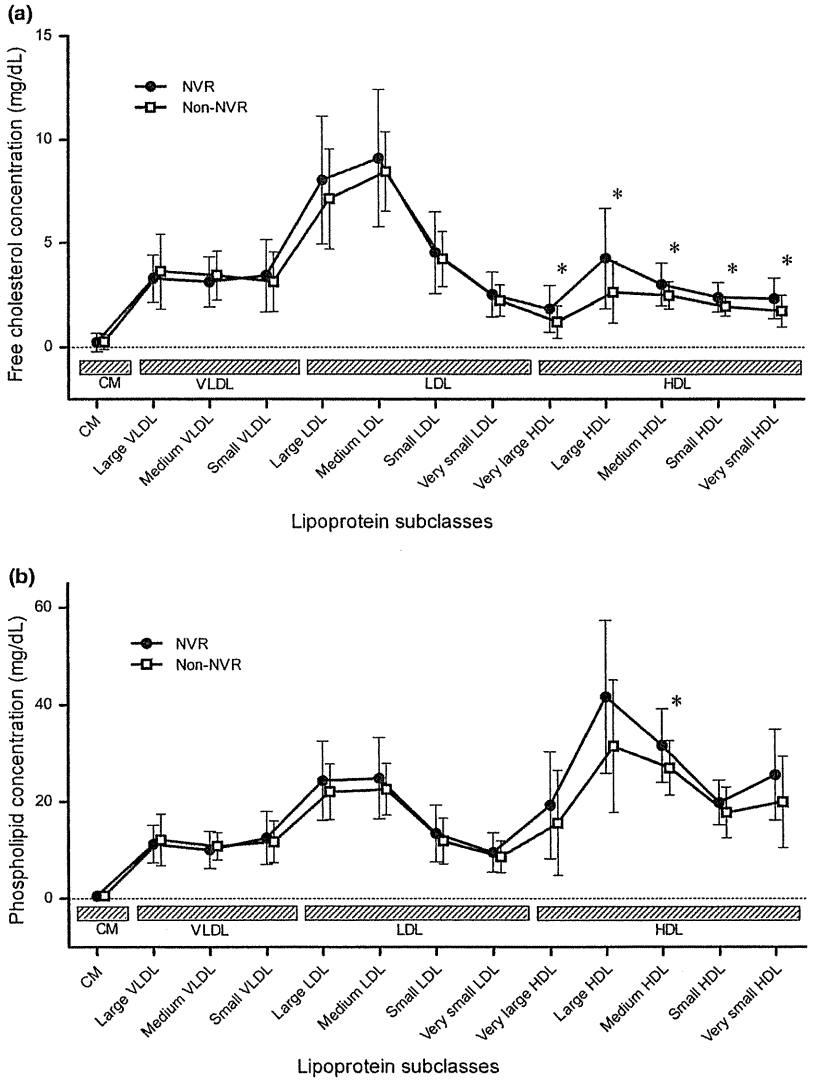

Fig. 1 Comparison of (a) free cholesterol and (b) phospholipid concentrations in lipoprotein subclasses between the nonvirological response (NVR) group and non-NVR group. The values are shown as the mean ± standard deviation (SD). CM, chylomicron (>70 nm in diameter); VLDL, very low-density lipoprotein (30–70 nm); LDL, low-density lipoprotein (16–30 nm); HDL, high-density lipoprotein (7–16 nm). *Subclass in which significant difference was observed between the NVR and non-NVR groups.

Table 2 Profiles of serum lipid levels in HDL subclasses

	Lipid concentrations (mg/dL)		
	NVR (n = 12)	Non-NVR (n = 43)	P
Phospholipid concentrations			
Very large HDL	19.3 ± 11.1	15.6 ± 10.8	0.306
Large HDL	41.6 ± 15.8	31.5 ± 13.7	0.070
Medium HDL	31.6 ± 7.6	27.0 ± 5.6	0.025
Small HDL	19.8 ± 4.6	17.7 ± 5.3	0.219
Very small HDL	25.6 ± 9.4	19.9 ± 9.4	0.050
Total HDL	137.9 ± 38.3	111.7 ± 24.6	0.006
Total lipoproteins	244.5 ± 54.7	212.0 ± 31.1	0.010
Free cholesterol concentrations			
Very large HDL	1.83 ± 1.12	1.20 ± 0.78	0.020
Large HDL	4.26 ± 2.43	2.63 ± 1.47	0.014
Medium HDL	3.01 ± 1.02	2.47 ± 0.65	0.031
Small HDL	2.39 ± 0.71	1.95 ± 0.47	0.013
Very small HDL	2.33 ± 0.96	1.73 ± 0.76	0.021
Total HDL	13.8 ± 5.1	10.0 ± 3.0	0.002
Total lipoproteins	48.1 ± 12.8	42.5 ± 7.39	0.056
Triglyceride concentrations			
Very large HDL	2.0 ± 1.0	1.9 ± 1.5	0.427
Large HDL	6.4 ± 3.6	5.6 ± 3.7	0.539
Medium HDL	5.0 ± 1.5	5.2 ± 1.9	0.684
Small HDL	3.2 ± 1.1	3.3 ± 1.1	0.852
Very small HDL	3.1 ± 0.8	3.0 ± 0.7	0.681
Total HDL	19.7 ± 6.2	19.6 ± 7.3	0.776
Total lipoproteins	97.4 ± 27.4	99.7 ± 30.2	0.935
Total cholesterol concentrations			
Very large HDL	5.2 ± 3.2	4.4 ± 2.7	0.367
Large HDL	17.2 ± 11.2	13.1 ± 7.2	0.229
Medium HDL	15.2 ± 5.6	13.7 ± 3.6	0.249
Small HDL	10.7 ± 4.1	10.0 ± 2.1	0.389
Very small HDL	9.0 ± 2.5	7.9 ± 1.6	0.071
Total HDL	57.4 ± 22.5	49.0 ± 12.2	0.165
Total lipoproteins	163.2 ± 39.2	166.9 ± 27.5	0.708

The values are shown as the mean ± standard deviation (SD). NVR, nonvirological response to pegylated interferon plus ribavirin combination therapy; HDL, high-density lipoprotein (7–16 nm in diameter).

No significant differences in the serum concentration of TG and the total cholesterol levels in all the lipoprotein subclasses were observed between the NVR and non-NVR groups (Table 2).

DISCUSSION

This study demonstrated that the serum PL and FC levels in the HDL fraction were significantly elevated in the NVR group compared with the values in the non-NVR group, before PEG-IFN-RBV combination therapy. HDL plays a key role in transporting cholesterol from the peripheral tissues to hepatocytes via scavenger receptor class B type I (SR-BI), a receptor for both HDL and HCV. Several laboratories have reported the infectivity of retroviral pseudoparticles bearing HCV E1E2 gps (HCVpp) [16–18]. HDL reportedly stimulates HCVpp entry into human hepatocarcinoma target cells [19–24], and this enhancement of HCVpp infection involves a complex interplay between the hypervariable region of HCV E2 protein, SR-BI, and HDL [19,23]. Nevertheless, the mechanism by which HDL increases HCV cell entry is not fully understood. Several studies have examined the enhancement of HCV infectivity by the apolipoproteins that constitute HDL [24–26]. Lipid-free apoA-I and apoA-II proteins, the major HDL apolipoproteins, had no effect on HCVpp entry despite their weak but real binding capacity to SR-BI [27,28]. The functional role of HDLs in lipid transfer is dependent on the proper orientation of apoA-I associated with lipids [29]. No reports have discussed the direct association between HCV infectivity and the lipid component of